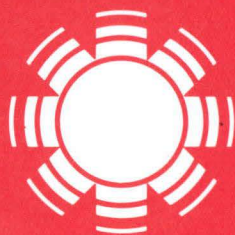


Optical Transparency of Inexpensive Salt Solutions for Construction of Density-Gradient Solar Ponds

John D. Webb



SERI

Solar Energy Research Institute

A Division of Midwest Research Institute

1617 Cole Boulevard
Golden, Colorado 80401

Operated for the
U.S. Department of Energy
under Contract No. EG-77-C-01-4042

SERI/RR-641-615

C.3

SERI/RR-641-615
UC CATEGORY: 59c

SOLAR ENERGY RESEARCH INSTITUTE
Solar Energy Information Center

OCT 28 1981

GOLDEN, COLORADO 80401

OPTICAL TRANSPARENCY OF
INEXPENSIVE SALT SOLUTIONS
FOR CONSTRUCTION OF DENSITY-
GRADIENT PONDS

JOHN D. WEBB

JULY 1981

PREPARED UNDER TASK NO. 1089.00

Solar Energy Research Institute

A Division of Midwest Research Institute

1617 Cole Boulevard
Golden, Colorado 80401

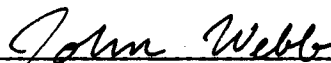
Prepared for the
U.S. Department of Energy
Contract No. EG-77-C-01-4042

SERIE part

PREFACE

This report outlines the progress that has been made to date in evaluating inexpensive salts for optical performance in density-gradient solar ponds. Work was carried out under the New Concepts Development Task (3141.99, FY 1980) in the Research Division of the Solar Energy Research Institute (SERI).

Helpful support and guidance given by Keith Masterson and David Benson during the development of a solar transmittance model used in this paper, and by Michael Edesess in developing the equations for pond design, is gratefully acknowledged. The author also thanks Mark Harris of the Monsanto Moundsville Laboratory and Navin D. Shah of the Electric Power Research Institute for providing the salt samples tested.



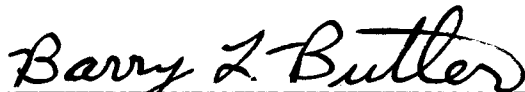
John Webb
Materials Research Branch

Approved for

SOLAR ENERGY RESEARCH INSTITUTE



Gordon Gross, Chief
Materials Research Branch



Barry Butler, Manager
General Research Division

SUMMARY

A major barrier to the commercialization of density-gradient solar ponds is the high cost of the salt used to produce the gradient. This cost is a function of purchase and transportation prices. Recently, new sources of salts, available in bulk as industrial waste, have been found near sites proposed for solar ponds. Before these salts can be accepted for use in solar ponds, their environmental impact, ability to create a stable gradient, and solar energy transmission when placed in solution must be investigated.

The purpose of this work was to establish a rapid laboratory measurement procedure to evaluate the solar transmittance of solutions of candidate salts and to estimate the solar transmittance of a given density gradient constructed using the candidate salt. This estimate is then used to calculate the necessary pond size to meet a given set of thermal demands. If the pond were to be constructed using the salt under evaluation, construction costs associated with the size estimates could then be balanced against the acquisition cost of the salt to select an optimum candidate.

One set of estimates for the performance of a flue gas desulfurization (FGD) by-product containing mainly sodium sulfate is presented. An error analysis of the measurement protocol, and an analysis of the effect of some trace contaminants on the transmittance of the salt solutions, are also presented. Suggestions to improve the accuracy of the measurement procedure, are included. The particular salt under study was found to be too low in transmittance as received to be useful, but several options exist for improving the performance of the salt solution in situ.

TABLE OF CONTENTS

	<u>Page</u>
1.0 Introduction.....	i
2.0 Apparatus.....	3
3.0 Procedure.....	5
3.1 Samples.....	5
3.2 Gravimetric and Chemical Analyses of Samples.....	5
3.3 Measurement of Optical Absorbance of Sample Solutions.....	5
3.4 An Attempt to Quantify Optical Measurement Errors.....	6
4.0 Prediction of Solar Energy Penetration into a Saline Concentration Gradient.....	7
4.1 Absorption of Light in a Homogenous Solution: An Ideal Case....	7
4.2 Actual Transmittance of Light in a Solar Pond.....	7
4.3 Solar Energy Penetration at Normal Incidence into a Nonscattering Gradient Pond.....	8
4.4 Effect of Salt Solution Transparency on Pond Design: A Basis for Determining Economic Acceptability of Alternate Salts.....	10
5.0 Results and Discussion.....	13
5.1 Gravimetric and Chemical Analyses.....	13
5.2 Discussion of Analytical Results.....	13
5.3 Predicted Effect of Some Ionic Contaminants on Energy Transmission.....	15
5.4 Comparison of Energy Penetration in an Actual Pond to that Predicted for a Similar Gradient Constructed from a Candidate Salt.....	16
5.5 Effect of the Solar Transmittance of a Salt Gradient on Pond Sizing.....	18
5.6 Spectral Transmittance of Miamisburg Pond Solution Samples.....	20
6.0 Error Analysis.....	27
7.0 Conclusions.....	35
8.0 Work in Progress.....	37
9.0 References.....	39
Appendix A: Program PON Output Listings.....	41

LIST OF FIGURES

	<u>Page</u>
5-1 Energy Penetration Profiles for Pure Water and for an FGD Salt Concentration Gradient Predicted Using Program PON.....	19
5-2 Dependence of Design Radius of a Typical Solar Pond on Average Energy Penetration.....	21
5-3 Transmittance and Absorbance Spectra of Miamisburg Pond Solution Sampled at 0.3-M Depth.....	23
5-4 Transmittance and Absorbance Spectra of Miamisburg Pond Solution Sampled at 1.2-M Depth.....	24
5-5 Transmittance and Absorbance Spectra of Miamisburg Pond Solution Sampled at 3.0-M Depth.....	25
6-1 Spectra of Boiled, Deionized Water and Air-Saturated, Deionized Water vs. Boiled, Deionized Water as a Reference.....	28

LIST OF TABLES

	<u>Page</u>
4-1 Solar Irradiance and Water Extinction Coefficients Data Used in the PON Program.....	11
5-1 Samples Received for Analysis.....	13
5-2 Results of Gravimetric Analyses.....	13
5-3 Results of Chemical Analyses.....	14
5-4 Gram Extinction Coefficients (Base e) Measured for Cu^{+2} and Fe^{+3} at pH of 4.0, in L/g-cm.....	15
5-5 Gram Extinction Coefficients (Base e) Measured for Candidate Solar Pond Salts, in L/g-cm $\times 10^4$	17
5-6 Concentration Profile of Evaporating Pond Salt Assumed for Energy Penetration Comparison to OSU Pond.....	18
5-7 Concentration Profile of Evaporating Pond Salt Assumed for Pond Design Analysis.....	20
6-1 Selected Constraints for Error Analysis Utilizing Eq. 6-8.....	31
6-2 Error in Spectral Intensity, I_1 , Predicted at a Depth of One Meter for a Pond Having the EPS Concentration Gradient Given in Table 5-6.....	32
6-3 Sensitivity of Predicted Solar Energy Transmitted to the Storage Layer of an EPS Solar Pond to a 1% Error in Laboratory-Measured Solution Transmittance.....	33
6-4 Error Boundaries on Program PON Predictions.....	34

NOMENCLATURE

FGD	flue gas desulfurization
$A(\lambda, \ell, c)$	total optical absorption by n species in a homogeneous solution with optical path length ℓ , at wavelength λ , as a function of the concentration c of each species
λ	wavelength, microns
ℓ	optical path length, cm
c_n	concentration of the n th species in solution, g/L
ϵ_n	gram extinction coefficient for the n th species in solution, L/g-cm
$I_o(\lambda)$	incident irradiance, $W/m^2-\mu m$
$I(\lambda)$	irradiance passing through a sample of optical path length ℓ , $W/m^2-\mu m$
$I_a(\lambda)$	irradiance absorbed in a sample of path length ℓ , $W/m^2-\mu m$
d	depth in solar pond, cm
θ_2	angle from vertical of light passing through solar pond, degrees
θ_1	angle from vertical of light incident on pond, degrees
n_1	refractive index of air at pond surface
n_2	refractive index of solution at pond surface
Δd_j	j th finite pond depth element for incremental analysis, cm
E_o	total available solar flux, W/m^2
$I_j(\lambda)$	irradiance penetrating j depth increments, W/m^2
E_{aj}	solar flux absorbed in j depth increments, W/m^2
E_a	total solar flux absorbed in j depth increments, W/m^2
P_t	percentage of available solar energy absorbed in j depth increments
r	design radius of solar pond necessary to meet a given thermal demand, m
ΔT	year-round average difference required between pond storage layer and ambient temperatures, $^{\circ}C$
\bar{L}	year-round average thermal demand to be met, W
\bar{E}_p	year-round average solar energy penetrating to the pond storage layer, W/m^2
\bar{E}_o	year-round average insolation available at pond surface, W/m^2
f	year-round average surface reflection loss fraction computed for the latitude of the pond

NOMENCLATURE (concluded)

GEC	gram extinction coefficient
EPS	evaporating pond salt
T_n	transmittance fraction predicted for species n at a given wavelength
c_{sn}	concentration of species n in solution, g/L
l_{sn}	effective path length of sample containing species n, cm
ΔI_1	error in irradiance predicted to penetrate to depth Δd_1 in a pond, a function of assumed pond and measured sample parameters and sample measurement errors, $W/m^2-\mu m$
ΔT_n	estimated error in spectrophotometrically measured transmission fraction of pond solution species n
$\Delta E_{T_n}(1)$	error in energy predicted to penetrate to depth Δd_1 in a pond, caused by errors in measuring the transmittance of all n species
$\Delta E_{max}(1)$	maximum error in energy predicted to penetrate to depth Δd_1 in a pond, caused by errors in measuring the transmittance of all n species
$\Delta E_{prob}(1)$	most probable error in energy predicted to penetrate to depth Δd_1 in a pond, caused by errors in measuring the transmittance of all n species

SECTION 1.0

INTRODUCTION

Salts for use in producing density gradients to stabilize solar ponds must meet four basic criteria:

- Solubility in water must increase with temperature;
- Salt must be readily available in bulk;
- Cost must be low; and
- Optical transparency of aqueous solutions of the salt must be high, particularly in the visible region of the solar spectrum.

Edesess et al. (1979) have identified salts that may satisfy the first three criteria listed above. These salts are available as waste from industrial processes such as ocean water desalination and flue gas desulfurization (FGD). The major components of such wastes are chlorides and sulfates of sodium and magnesium.

Current models for predicting solar pond performance use only the solar absorbance spectrum of pure water to determine energy penetration to the storage layer of the hypothetical pond. However, the hydrated salt ions may absorb solar radiation to some extent, and even purified salts may contain small percentages of transition metal ions, insoluble fines, or organic matter. Industrial waste salts may contain significant levels of these impurities, and further contamination may be present in the water used to fill the pond. All of these factors will act in concert to reduce energy penetration to the storage layer of a pond through absorption or scattering of solar radiation passing through the density gradient of the pond. If the losses are significant, the pond must be designed with a greater surface area to meet thermal demand while maintaining the design temperature in the storage layer.

The purpose of this work was to establish a laboratory procedure for evaluating the optical performance of candidate salts for use in solar ponds, including ponds planned to be built at the permanent SERI field testing site. Optical extinction coefficients for such salts were obtained at discrete wavelengths spanning the solar ultraviolet, visible, and near-infrared spectra. A simple digital model was constructed, which made use of these data to predict solar energy penetration into a hypothetical pond having a given concentration profile of the salt under study. To determine the effect of salt type on the radius of a pond designed to meet a given set of thermal load requirements, results of this analysis, expressed as energy deposition rate per square unit as a function of depth, were input to a solar pond design equation developed by Edesess et al. (1979). Results of this analysis are presented in Sec. 5.5.

SERIO 

SECTION 2.0

APPARATUS

Beckman Model DK-2 (wavelength range 270-2800 nm) and Perkin-Elmer Model 340 (190-2500 nm) spectrophotometers were used to make the absorbance measurements. The sample and reference solutions were contained in quartz single-pass cells having path lengths of 1, 5, and 10 cm.

The sulfate content of the FGD salts was determined with a Hach colorimetric chemical analyzer. Trace elemental analysis of the samples was performed using a Perkin-Elmer Model 303 atomic absorption spectrophotometer.

Analyses for density, percent solids, and percent volatiles were carried out using a Mettler analytical balance with a precision of 0.1 mg, and a Blue M drying oven set at 100°C.

SERIO 

SECTION 3.0

PROCEDURE

3.1 SAMPLES

Four samples of FGD salts and salt solutions were received from KVB Engineering Company through the Electric Power Research Institute (EPRI). The sample materials were by-products from an experimental dry scrubber at a coal-fired electric generating plant in Utah. Additional liquid samples, taken from 0.3-, 1.2-, and 3-m levels of a stratified solar pond at Miamisburg, Ohio, were received at SERI. The salinity gradient of the pond was established using USP grade sodium chloride dissolved in local water.

3.2 GRAVIMETRIC AND CHEMICAL ANALYSES OF SAMPLES

The two solid samples of FGD salts received were analyzed for percent volatiles by baking at 100°C for 24 h. To remove the fly ash, which appeared to constitute much of the solid samples, 22.853-g portions of each sample were dispersed in 100 mL of deionized water, and the resultant slurries were vacuum filtered through fast, preweighed filter paper dishes. The residues were washed with small amounts of deionized water totaling 100 mL. The papers and filtrate were dried as described above and weighed to estimate the percentage of insoluble matter in the solid samples.

The supernatant solutions and the two sample solutions of dissolved salt were analyzed for percent solids by drying weighed portions for 24 h in a drying oven set at 100°C. Liquid sample density was determined by weighing pipetted volumes of 2 mL of sample to a precision of 0.1 mg at 25°C. The four FGD solutions, as well as the three Miamisburg pond samples, were retained for spectrophotometric and chemical analyses.

The samples of FGD effluent and evaporating pond solutions were tested for sulfate content using a Hach colorimetric chemical analyzer. These samples were also tested for iron and copper content using a Perkin-Elmer Model 303 atomic absorption spectrophotometer.

Sodium chloride content of the Miamisburg samples was determined by correlating specific gravity measurements taken at Miamisburg with literature values (Weast 1969) for sodium chloride solutions. The Miamisburg samples were also analyzed for iron, copper, and magnesium content by means of atomic absorption spectrophotometry.

3.3 MEASUREMENT OF OPTICAL ABSORBANCE OF SAMPLE SOLUTIONS

The four FGD sample solutions were analyzed for spectral absorbance under a contract to the Denver Research Institute. Quartz cells of 10-, 5-, and 1-cm path lengths were used to contain the sample solutions. For the 5- and 10-cm sample cells, a 1-cm cell containing boiled, deionized water was used as a

reference standard. For the 1-cm sample cell, a 1-cm reference cell containing spectrophotometric grade carbon tetrachloride was used.

Three sets of plots of absorbance versus wavelength, corresponding to each of the three sample cell lengths, were generated for each of the FGD samples. Each set contained six absorbance plots, one for each of the samples, plus one plot taken with both cells empty and another taken with the cells filled with boiled, deionized water. For the 1-cm sample cell, a baseline scan was run using water in the sample cell and carbon tetrachloride in the reference cell.

The Miamisburg salt solutions were analyzed for spectral absorbance at SERI using a Perkin-Elmer Model 340 spectrophotometer covering a range of 190-2500 nm. Ten-cm quartz samples and reference cells were used. The reference cell contained boiled, deionized water. Solutions containing 100-ppm magnesium, 50-ppm copper, and 5-ppm iron were also analyzed in this fashion.

3.4 AN ATTEMPT TO QUANTIFY OPTICAL MEASUREMENT ERRORS

To determine the effect of dissolved air on the spectrophotometric analysis, deionized water saturated with air by bubbling for 10 min, was analyzed on the Perkin-Elmer instrument. The cell containing air-saturated water was agitated ultrasonically to coalesce the remaining air bubbles. Miamisburg samples from 0.3 and 1.2 m were also boiled for spectral analysis in this manner. An absorbance plot for the 0.3 m sample was obtained. A white precipitate formed when the 1.2 m sample was boiled, precluding any spectral analysis.

To determine the effect of possible errors in sample cell positioning on measured transmittance, two 10-cm cells containing deaerated water were placed into the cell holder in the spectrophotometer sample compartment. With the reference cell fixed, the sample cell was manually rotated about its long axis as far as the cell holder would permit (about 45°), with the instrument grating set to 550 nm. The variations in the indicated transmittance fraction introduced by these variations in sample cell position were recorded. Results of the procedures appear in the section on error analysis, Sec. 6.0.

SECTION 4.0

PREDICTION OF SOLAR ENERGY PENETRATION INTO A SALINE CONCENTRATION GRADIENT

4.1 ABSORPTION OF LIGHT IN A HOMOGENOUS SOLUTION: AN IDEAL CASE

Absorption of light by any species in a homogenous solution is a function of wavelength λ , optical path length ℓ , and species concentration c . When n light-absorbing species are present in a solution, an expression for the total absorption of the solution can be written as follows:

$$A(\lambda, \ell, c) = A_1(\lambda, \ell, c_1) + A_2(\lambda, \ell, c_2) + \dots + A_n(\lambda, \ell, c_n) \quad , \quad (4-1)$$

The Lambert-Beer expression for absorbance may be used to reduce the right-hand portion of Eq. 4-1:

$$\begin{aligned} A(\lambda, \ell, c) &= \epsilon_1(\lambda)\ell c_1 + \epsilon_2(\lambda)\ell c_2 + \dots + \epsilon_n(\lambda)\ell c_n \\ &= \ell(\epsilon_1 c_1 + \epsilon_2 c_2 + \dots + \epsilon_n c_n) \quad , \end{aligned} \quad (4-2)$$

where $\epsilon_n(\lambda)$ is the extinction coefficient for species n , which exists at concentration c_n in the solution. If these variables are known for all n species at a given wavelength, the total absorbance at that wavelength can be calculated. If all light attenuation observed in the sample is caused by absorption, i.e., no scattering or other nonlinear light attenuation occurs, the total absorbance can be related to the ratio of incident and exiting irradiance, $[I_0(\lambda)/I(\lambda)]$, passing through a sample having an optical path length ℓ , as follows:

$$\ln [I_0(\lambda)/I(\lambda)] = A(\lambda, \ell, c) \quad , \quad (4-3)$$

or

$$I(\lambda) = I_0(\lambda) \exp [-A(\lambda, \ell, c)] \quad . \quad (4-4)$$

Defining the absorbed irradiance $I_a(\lambda)$ to equal $I_0(\lambda) - I(\lambda)$, the following equation for irradiance absorbed at a given wavelength can be written:

$$I_a(\lambda) = I_0(\lambda) (1 - \exp[-A(\lambda, \ell, c)]) \quad . \quad (4-5)$$

4.2 ACTUAL TRANSMITTANCE OF LIGHT IN A SOLAR POND

Equation 4-5 may be modified to include the effect of a concentration gradient by making the c_n in Eq. 4-2 functions of ℓ . However, it is difficult to use Eq. 4-5 to predict light transmission in an actual solar pond for several

reasons. One problem is that the direction and length of the optical path in a pond is difficult to define. Path length λ is related to depth d by the ratio:

$$\frac{d}{\cos \theta_2} = \lambda \quad , \quad (4-6)$$

where θ_2 is the angle that light passing through the pond makes with the vertical. θ_2 is in turn related to θ_1 , the angle of light incident on the pond, by Snell's law:

$$\frac{n_1}{n_2} = \frac{\sin \theta_2}{\sin \theta_1} \quad , \quad (4-7)$$

where, in this case, n_1 and n_2 are the refractive indices of air and of the pond solution, respectively. Since these indices depend on wavelength, the path of light through the pond, as defined by θ_2 and d , also varies with the wavelength of the incident light. For example, Querry et al. (1977) have shown that refractive indices for pure and saline water may vary from 1.15 to 1.55 over the range of 2-20 microns, resulting in a variation of up to 15° in θ_2 over this range for an incidence angle θ_1 of 45°. Another complication is that I_0 in Eq. 4-5 is always less than the intensity of light as measured above the pond surface because of losses from surface reflection. Reflective losses are also wavelength-dependent, and they become significant at high angles of incidence. Finally, θ varies because of waves on the pond surface. For these reasons, mathematical analysis of light penetration into an actual solar pond would present a complex problem, even if the effects of light scattering were not considered.

4.3 SOLAR ENERGY PENETRATION AT NORMAL INCIDENCE INTO A NONSCATTERING GRADIENT POND

To circumvent the complicating difficulties discussed in Sec. 4.2, a simple algorithm was developed for comparing the effects of light absorption by candidate solar pond solutes on the optical performance of an idealized pond. In the model, normal incidence of light onto the pond ($\theta_1 = 0$) was assumed. In this case, Eq. 4-6 reduces to $d = \lambda$, θ_2 becomes zero, and reflective losses are minimized. Under these conditions, Eq. 4-5 may be written in terms of a finite depth element Δd , chosen so that the concentrations of the absorbing species do not change significantly over the length of the element:

$$I_j(\lambda) = I_{j-1}(\lambda) \exp \left[-\Delta d_j (\epsilon_1(\lambda)c_1(d) + \epsilon_2(\lambda)c_2(d) \dots + \epsilon_n(\lambda)c_n(d)) \right] \quad . \quad (4-8)$$

To obtain the total energy E_o available from the incident sunlight, the following relation

$$E_o = \int_{\lambda_1}^{\lambda_2} I_o(\lambda) d\lambda \quad (4-9)$$

may be employed, assuming that reflective losses are negligible for the normal incidence case.

The limits λ_1 and λ_2 were chosen as 0.3 and 2.5 microns, respectively, to encompass about 99% of the available solar flux.

The energy absorbed in the j th depth increment can be obtained by a similar integration of Eq. 4-8:

$$E_{aj} = \int_{\lambda_1}^{\lambda_2} (I_{j-1}(\lambda) - I_j(\lambda)) d\lambda \quad (4-10)$$

The cumulative energy absorbed in j depth intervals, or through a depth equal to

$$\sum_i^j \Delta d_j,$$

can be expressed as:

$$E_a = \sum_1^j E_{aj} \quad (4-11)$$

For convenience in evaluating Eq. 4-11 numerically, depth increment Δd_j in Eq. 4-8 may be varied as a step function of pond depth d . The depth increments used should be minimized until E_a (total) converges to within acceptable levels. For improved accuracy, $C_1 \dots C_n$ can be taken at the midpoint of the Δd_j .

The percentage of the total available solar energy absorbed in j depth increments can now be calculated:

$$P_t = 100 E_a / E_o \quad (4-12)$$

A software routine (PON), was developed to evaluate Eqs. 4-9, 4-11, and 4-12 for the case of normal incidence of sunlight on a pond with a known salt concentration gradient. It was assumed that the concentration of all absorbing species in the pond was directly proportional to either the concentration of the dissolved salt or to that of the solvent water. By making this assumption, Eq. 4-1 is truncated at $n = 2$. $I_o(\lambda)$ was approximated by 88 ordered pairs (λ, I_o) taken from an Air Mass 1.5 solar spectrum developed at NASA-Lewis (Brandhorst et al. 1977). Thirty-one ordered pairs (λ, ϵ_2) of data taken both at SERI and from the International Critical Tables (Washburn 1929) were used

to approximate $\epsilon_2(\lambda)$ for water. Measurements on water made at SERI showed good agreement with the ICT values, but the range of the data collected was limited by the extreme variations in the $\epsilon_2(\lambda)$ for water. Both sets of data were stored externally to the program, and are reproduced in Table 4-1. The interactive program was written to accept user inputs of salt extinction coefficient versus wavelength, and of salt and water concentrations versus depth. A subroutine was written to perform a linear interpolation yielding the appropriate independent variable when values of wavelength or depth falling between the points supplied were encountered during compilation. Depth increment Δd could be reset at a depth d specified by the user.

An inspection of the extinction coefficient versus wavelength data revealed that the major contributor to solution absorbance at wavelengths greater than 800 nm is water, since even in a saturated salt solution the concentration of water will be several times greater than that of the salt. Above 1100 nm, data acquisition became impossible because of the strong absorbance of water in this region. An assumption was made that the salt extinction coefficient $\epsilon_1(\lambda)$ remains constant, and that it was small compared to that of water, throughout the interval 1100-2500 nm. This enabled integration to extend over this interval, making use of literature values for the extinction coefficients of water, and eliminating the need to measure extinction coefficients for the salts in this region. Solutions to Eq. 4-12 were approximated numerically using the trapezoidal method. The wavelength range for integration was determined by a software scan of the optical data entered. The integration interval is selected by the user. Intervals of 10 nm were standard for integration between 300 and 2500 nm. A complete program listing is available on request.

4.4 EFFECT OF SALT SOLUTION TRANSPARENCY ON POND DESIGN: A BASIS FOR DETERMINING ECONOMIC ACCEPTABILITY OF ALTERNATE SALTS

To determine the effect of gradient transparency upon the design of a typical pond, the sizing equations developed by Edesess et al. (1979) were used. Optical transparency of the upper layers of the pond will determine the surface area of a pond designed to meet a given thermal demand.

The sizing equation for the radius r of the circular pond under the specific conditions set forth in the work referenced above is:

$$r = \frac{2.2 \Delta T + [4.84 \Delta T^2 + \bar{L} (0.3183 \bar{E}_p - 0.1592 \Delta T)]^{1/2}}{\bar{E}_p - 0.5 \Delta T}, \quad (4-13)$$

where ΔT is the average difference required between the pond storage layer and ambient temperatures ($^{\circ}\text{C}$), \bar{L} is the average thermal demand to be met, and \bar{E}_p is the average solar energy penetrating to the pond storage layer (r in meters, \bar{L} in watts, and \bar{E}_p in watts per square meter). This equation was developed assuming surface heat losses of $0.4 \text{ W/m}^2\text{-}^{\circ}\text{C}$, edge losses of $2.2 \text{ W/}^{\circ}\text{C}$ per meter of pond perimeter, and bottom heat losses of $0.1 \text{ W/m}^2\text{-}^{\circ}\text{C}$.

Table 4-1. SOLAR IRRADIANCE AND WATER EXTINCTION COEFFICIENT DATA USED IN THE PON PROGRAM

PON FILE NAME: "SOLS"			PON FILE NAME: "WATER"		
Wavelength (nm)	Solar Irradiance ^a (W/m ² -μm)	Wavelength (nm)	Solar Irradiance (W/m ² -μm)	Wavelength (nm)	Extinction Coefficient (L/g-cm)
295.	0.	720.	1133.83	295.	0.200E-05
305.	1.32	728.	974.3	320.	0.160E-05
315.	20.96	730.	1110.93	330.	0.150E-05
325.	113.48	740.	1086.44	340.	0.120E-05
335.	182.43	750.	1070.44	350.	0.930E-06
345.	234.43	762.	733.08	360.	0.640E-06
355.	286.01	770.	1036.01	380.	0.260E-06
365.	355.08	780.	1018.42	400.	0.130E-06
375.	386.8	790.	1003.58	450.	0.160E-06 ^b
385.	381.78	800.	988.11	500.	0.170E-06 ^b
395.	492.18	806.	860.28	550.	0.300E-06 ^b
406.	751.72	825.	932.74	570.	0.300E-06 ^b
415.	822.45	830.	923.87	580.	0.400E-06 ^b
425.	842.26	847.	407.11	590.	0.780E-06 ^b
435.	890.55	860.	857.46	600.	0.150E-05 ^b
445.	1077.07	870.	843.02	700.	0.375E-05 ^b
455.	1162.43	875.	835.1	750.	0.240E-04 ^b
465.	1180.61	888.	817.12	800.	0.200E-04 ^b
475.	1212.72	900.	807.83	900.	0.610E-04
485.	1180.43	908.	793.87	940.	0.168E-03
495.	1253.83	915.	778.97	980.	0.583E-03
505.	1242.28	925.	217.12	1065.	0.130E-03
515.	1211.01	930.	163.72	1100.	0.190E-03
525.	1244.87	940.	249.12	1130.	0.600E-03 ^b
535.	1299.51	950.	231.3	1170.	0.110E-02 ^b
545.	1273.47	955.	255.61	1210.	0.130E-02 ^b
555.	1276.14	965.	279.69	1281.	0.120E-02 ^b
565.	1277.74	975.	529.64	1400.	0.310E-02 ^b
575.	1292.51	985.	496.64	1450.	0.200E-01 ^b
585.	1284.55	1018.	585.03	1500.	0.300E-01 ^b
595.	1262.61	1082.	486.2	1677.	0.520E-02 ^b
605.	1261.79	1094.	448.74	1750.	0.750E-02 ^b
615.	1255.43	1098.	486.72	1900.	0.320E-01 ^b
625.	1240.19	1101.	500.57	1956.	0.120E+00 ^b
635.	1243.79	1128.	100.86	2000.	0.700E-01 ^b
645.	1233.96	1193.	424.85	2237.	0.200E-01 ^b
655.	1182.32	1288.	345.69	2400.	0.400E-01 ^b
665.	1228.4	1384.	2.42	2600.	0.530E-02 ^b
675.	1210.08	1457.	67.14		
685.	1200.72	1599.	220.46		
695.	1181.24	1862.	2.01		
698.	973.53	2014.	80.01		
700.	1173.31	2537.	2.59		
710.	1152.7				

^aSolar irradiance data (Air Mass 1.5) were taken from Brandhorst et al. (1977).

^bTaken from Washburn et al. (1929).

The remaining extinction coefficient data were generated at SERI.

Assuming that significant shifts in relative solar spectral intensities do not occur seasonally, \bar{E}_p may be approximated as follows, given E_o and $E_a(\text{total})$:

$$\bar{E}_p = f\bar{E}_o \frac{[E_o - E_a(\text{total})]}{E_o}, \quad (4-14)$$

where \bar{E}_o is the seasonally averaged available insolation (W/m^2), and f is the seasonally averaged fraction of energy lost through reflection at the pond surface for the latitude of the pond.

A complete listing of terms is given in the Nomenclature at the beginning of this report.

SECTION 5.0

RESULTS AND DISCUSSION

5.1 GRAVIMETRIC AND CHEMICAL ANALYSES

Descriptions of the solid and liquid samples of salt-containing material received for analysis, as well as the analytical results, are given in Tables 5-1, 5-2, and 5-3..

Table 5-1. SAMPLES RECEIVED FOR ANALYSIS

Sample Description	Sample Labels
2 cans grey powder	Test #9 - Trona & Fly Ash Test #15 - Nahcolite & Fly Ash
2 bottles clear liquid	Scrubber effluent pond Scrubber evaporating pond
3 bottles clear liquid	Miamisburg - 0.3 m depth Miamisburg - 1.2 m depth Miamisburg - 3.0 m depth

Table 5-2. RESULTS OF GRAVIMETRIC ANALYSES

	(%) Volatiles at 100°C	(%) Insolubles at 25°C
Test #9 (powder)	0.94	67.9
Test #15 (powder)	1.06	66.5
	(%) Solids at 100°C	Density (g/mL) at 25°C
Test #9 Extract (liquid)	3.58	1.026
Test #15 Extract	3.75	1.023
Effluent Pond	3.58	1.025
Evap. Pond	9.96	1.088
Miamisburg 0.3 m	1.40	1.010
Miamisburg 1.2 m	4.50	1.032
Miamisburg 3 m	18.9	1.141

5.2 DISCUSSION OF ANALYTICAL RESULTS

The FGD powder samples received were roughly two-thirds fly ash by weight. Filtration of extracts from these samples did not remove all of the insoluble ash, which contains considerable amounts of iron, very little of which would

Table 5-3. RESULTS OF CHEMICAL ANALYSES

Sample	[Cu ⁺²] (ppm)	[Fe ⁺³] (ppm)	[Mg ⁺²] (ppm)	SO ₄ ⁻² as Na ₂ SO ₄ (% dry wt.)	(pH) As Received
Test #9 Extract	0.04	0.00 ^a	--	--	10.5
Test #15 Extract	0.12	0.13 ^a	--	--	10.9
Effluent Pond	0.16	1.26 ^a	--	96	8.6
Evap. Pond	0.15	0.00	--	92	4.1
Miamisburg 0.3 m	0.00	0.00	17.9	--	8.2
Miamisburg 1.2 m	0.30	0.00	32.2	--	8.3
Miamisburg 3 m	1.00	0.70	37.3	--	7.3

^aSolid residue in these extracts contained considerable amounts of iron. The results shown apply to the supernatant liquid.

be soluble at the pH levels observed for the extracts. The high pH measured for the extracts indicates the presence of unreacted sodium carbonate in the powder samples. The effluent and evaporating pond solutes were nearly pure Na_2SO_4 and contained small but measurable quantities of copper. The probable sources of the increasing concentrations of copper ions found in the lower layers of the Miamisburg pond were the copper salts that were added to the pond as a bactericide, and a copper heat exchanger, which rapidly corroded once in service. The concentration of iron in the lowest layer of the pond is probably enhanced by the decreasing pH gradient present in the pond, and by the high concentration of chloride ions in this layer, which would tend to complex the ferric ions. The iron found may have been introduced originally in the well water used to fill the pond, or in the salt used to construct the density gradient. It is uncertain whether the concentrations of iron and copper found represent ionic species or finely divided hydroxide precipitates in the sample solutions.

5.3 PREDICTED EFFECT OF SOME IONIC CONTAMINANTS ON ENERGY TRANSMITTANCE

Iron and copper ion concentrations were investigated, because the presence of these chromophores in significant quantity could reduce light transmittance through a solar pond. Spectra were collected as described in the previous section on dilute aqueous solutions of iron, copper, and magnesium ions. Magnesium ions at 100 ppm concentration show insignificant absorbance relative to that of water throughout the visible region. Iron and copper both show absorption in the blue and ultraviolet region, with copper also showing some absorption in the red and near infrared region. Extinction coefficients for iron and copper calculated from these spectra, covering a range of 300-850 nm, are given in Table 5-4.

Table 5-4. GRAM EXTINCTION COEFFICIENTS (Base e) MEASURED FOR Cu^{+2} AND Fe^{+3} AT pH OF 4.0, IN L/g-cm

Cu^{+2}		Fe^{+3}	
Wavelength (nm)	Extinction Coefficient	Wavelength (nm)	Extinction Coefficient
300	3.79	300	90+
340	0.385	330	90+
390	0.000	400	5.41
610	0.000	420	1.38
850	0.446	500	0.000
		850	0.000

To estimate the optical effect of various levels of these potential contaminants in solar ponds, the PON program was used to calculate the transmittance losses associated with introduction of small amounts of Cu^{+2} and Fe^{+3} into an

element of pure water one meter in depth. In most stratified ponds, sunlight must penetrate at least to this depth to reach the storage zone. It was found that the presence of 5-ppm Cu^{+2} would reduce transmittance through a 1-meter path of otherwise pure water by 1%. A similar reduction would occur if as little as 0.1-ppm Fe^{+3} were present. These estimates are conservative because the results listed in Table 5-4 were taken in the absence of complexing ligands. In a pond made up of NaCl for example, one would expect to find more intense absorption, resulting from formation of the chloride coordination complexes of these transition metal ions, especially at low pH. Therefore, concentration of these and other transition metal ions in gradient ponds should be kept to a minimum. Several conclusions regarding the results of the chemical analyses reported in Table 5-3 can now be made. First, concentrations of iron and copper in the upper portion of the Miamisburg pond are insufficient to reduce pond performance significantly. The pH of the pond is high enough to drive these ions out of solution as hydroxides, and the low concentrations measured indicate that any resulting suspension has settled.

In the FGD salt solutions, significant amounts of iron were detected, but the pH of the solutions, with the exception of the evaporating pond solution, was also high enough that the iron could only exist as the hydroxide precipitate. The erratic atomic absorption measurements made on the alkaline samples support this hypothesis. The iron-containing residue had apparently settled out before reaching the evaporating pond; thus, no iron was found there. Finely divided ferric hydroxide in suspension has a yellowish tint, although it can be flocculated by boiling to give a red precipitate. The presence of such particulates may be a determining factor in the optical performance of the samples tested, and will be discussed in the Error Analysis, Sec. 6.0.

As noted in this section, boiling the Miamisburg samples taken at four and ten feet resulted in the formation of a white precipitate. This phenomenon, coupled with the high pH and magnesium levels observed for these samples (see Table 5-3), indicates that the well water used to make up the Miamisburg pond was high in bicarbonate hardness. Heating these samples evidently drove off carbon dioxide, raising the pH sufficiently to precipitate the magnesium as $\text{Mg}(\text{OH})_2$. Solubility product calculations based on the original concentration of Mg^{+2} and the original pH of the samples support this hypothesis.

5.4 COMPARISON OF ENERGY PENETRATION IN AN ACTUAL POND TO THAT PREDICTED FOR A SIMILAR GRADIENT CONSTRUCTED FROM A CANDIDATE SALT

In predicting the energy penetration through gradients of candidate salts, no attempt was made to break the total sample absorbances down into more than two components, i.e., water and solvated salt. By comparing the data in Tables 5-2 and 5-3 one can see that the concentration gradients of minor impurities roughly parallel the gradient measured for NaCl in the Miamisburg pond. Therefore, a gram (or overall) extinction coefficient (GEC), rather than the more commonly used molar coefficient, was developed to express the light-absorbing properties of solutions of the candidate salts. In Table 5-5 GEC coefficients are listed for the FGD salts, measured as described in the preceding section.

Table 5-5. GRAM EXTINCTION COEFFICIENTS (Base e) MEASURED FOR CANDIDATE SOLAR POND SALTS, IN $L/g\text{-cm} \times 10^4$

Wavelength (nm)	Pure Water	Evaporating Pond Salt	Effluent Pond Salt	Test #15 Salt	Test #9 Salt
300	0.019	20.0			
320	0.016	14.0	24.0	47.0	120.0
330	0.015	11.0	17.0	34.0	89
340	0.012	9.6	13.0	32.0	75.0
350	0.0093	7.9	8.8	31.0	67.0
360	0.0064	7.1	7.0	30.0	59.0
380	0.0026	4.6	4.2	19.0	39.0
400	0.0013	3.0	3.2	9.7	25.0
450	0.0016 ^a	1.5	1.9	2.9	9.6
550	0.0030 ^a	0.52	1.3	0.42	0.88
700	0.038 ^a	0.18	0.59	b	b
750	0.24 ^a	0.11	0.29	b	b
800	0.20 ^a	0.12	0.36	b	b
900	0.61	0.00	0.00	0.00	0.00
940	1.7	0.00	0.00	0.00	0.00
1065	1.3	0.21	0.63	0.00	0.63
1100	1.9	0.00	0.00	0.00	0.00

^aValue taken from Washburn (1929).

^bNegative result.

A comparison of these data with those presented for copper and iron in Table 5-4 reveals that on a gram basis, the candidate salts are generally intermediate in ultraviolet light absorbance between pure water and these transition metal ions. However, there is no direct correlation between copper or iron content of the candidate salts and the measured extinction coefficients. The zero and negative results are an indication of the difficulty of obtaining meaningful measurements of very low extinction coefficients. These difficulties are discussed in Sec. 6.0.

The evaporating pond salt (EPS) solution appeared to be the most likely candidate for solar pond usage, with reference to the data presented in Table 5-5. Therefore, the PON program was used to evaluate the energy penetration into a hypothetical pond having a concentration profile of similar solute as shown in Table 5-6. This profile was measured by Nielsen (1976) at the Ohio State University experimental pond.

The results of the PON energy penetration analysis performed on this EPS gradient and on pure water appear as Fig. 5-1. For comparison, energy penetration measurements made by Nielsen (1976) at the OSU pond using a submersible pyranometer are also plotted. It should be recalled that differences between program PON predictions and actual energy penetration measurements may arise from the assumptions made in developing the software routine, as well as from the sources of measurement error described by Nielsen. Also, the solar spectrum used by Nielsen in his analyses has less infrared content than does the NASA-Lewis spectrum used as input to PON.

Table 5-6. CONCENTRATION PROFILE OF EVAPORATING POND SALT ASSUMED FOR ENERGY-PENETRATION COMPARISON TO OSU POND

Depth (cm)	Salt Concentration (g/L)	Water Concentration (g/L)
0.0	25.5	995.5
43.0	25.5	995.5
100.0	171.1	969.5
230.0	197.3	963.4

The PON results indicate that a pond gradient constructed of EPS as shown in Table 5-6 would exhibit about 29% less energy penetration to the storage layer than did the OSU pond, and about 40% less energy penetration than would an equal depth of pure water. The effect of the increase in salt concentration at 43-cm depth can be clearly seen as an inflection point in the EPS curve presented in Fig. 5-1.

Output listings of the PON runs are reproduced in Appendix A.

5.5 EFFECT OF THE SOLAR TRANSMITTANCE OF A SALT GRADIENT ON SIZING A POND

An estimate of the economic advantage to be gained by replacing pure salts with inexpensive alternates requires calculating the effect of differences in solar transmission on pond design. As mentioned in the Introduction, any significant reduction of energy reaching the storage area of a pond will require a greater surface area to meet the thermal demand, as well as a higher construction cost. Such costs must be balanced against the savings afforded by the use of the alternate salt.

The salt concentration profile given in Table 5-6 for the OSU pond does not correspond to the gradient zone thickness assumed by Edesess et al. (1979) in developing their design equations (i.e., Eq. 4-15). For analysis by program PON, a concentration profile of EPS that matches the zone thicknesses implied in Eq. 4-15 was assumed. Concentrations at the zone boundaries were the same as those used previously. The resulting profile is given in Table 5-7.

Program PON was run to estimate the fraction of available solar energy that would penetrate such a gradient. At the depth of the storage layer of the design pond (150 cm), the value of the ratio $[E_0 - E_a(\text{total})]/E_0$ predicted by program PON was 0.17. This result can be substituted into Eq. 4-16, assuming a surface transmittance f of 0.97 and a seasonally averaged insolation \bar{E}_0 of 206 W/m^2 , to give an estimate for the seasonally averaged energy transmitted to the storage layer of the pond, \bar{E}_p , of 34 W/m^2 . Similarly, if the dissolved salt added nothing to the optical absorbance of the solvent water, a solar-transmittance fraction of 0.42 is predicted, resulting in an average energy

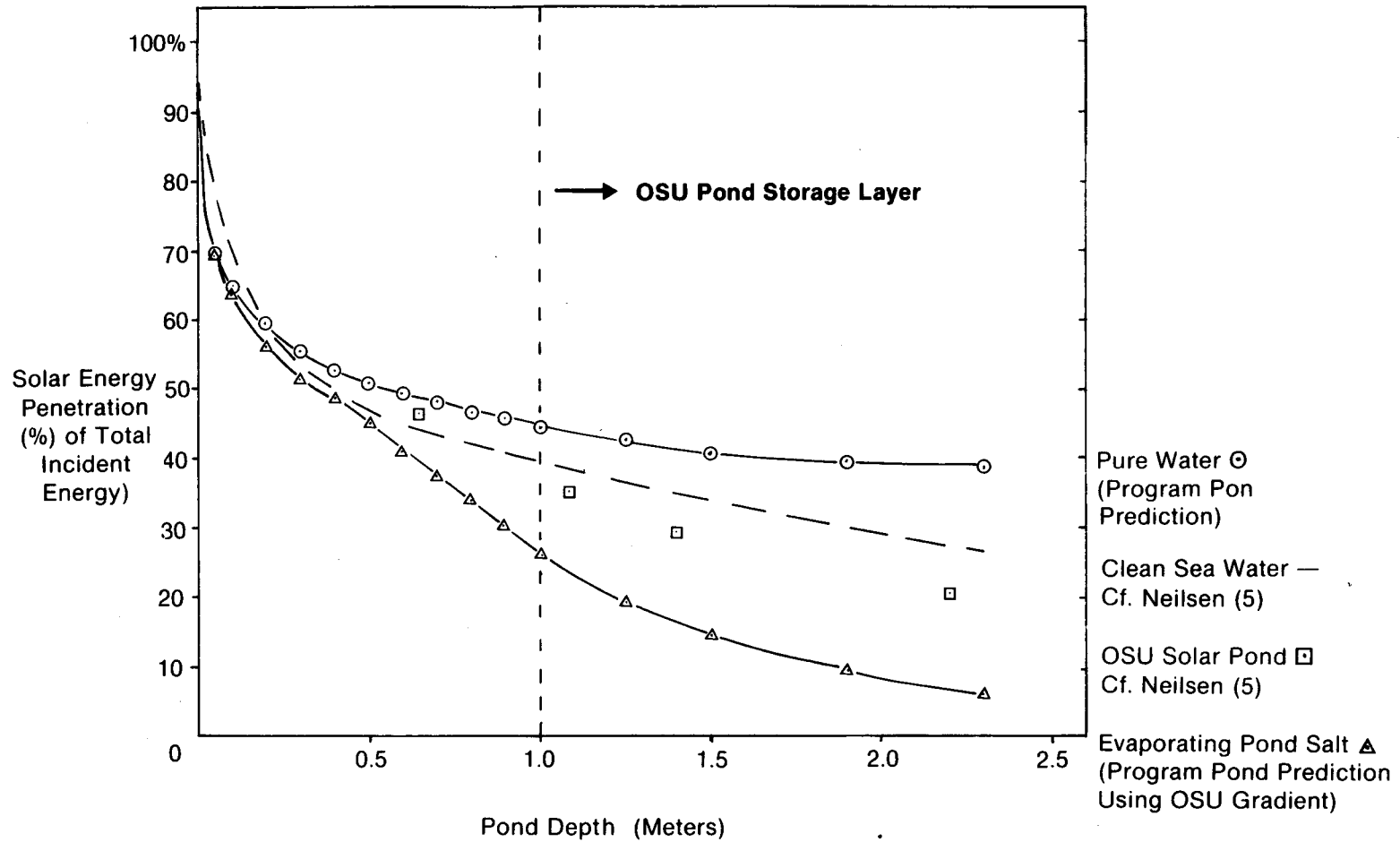


Figure 5-1. Energy Penetration Profiles for Pure Water and for an FGD Salt Concentration Gradient Predicted Using Program PON (Results obtained by Neilsen (5) are presented for comparison.)

Table 5-7. CONCENTRATION PROFILE OF EVAPORATING POND SALT ASSUMED FOR POND DESIGN ANALYSIS

Depth (cm)	Salt Concentration (g/L)	Water Concentration (g/L)
0.0	25.5	995.5
30.0	25.5	995.5
150.0	171.1	969.5
230.0	197.3	963.4

input of 84 W/m^2 to the storage layer. Edesess et al. (1979) assume an intermediate solar transmittance of 0.31 for a 150-cm deep gradient layer constructed of clean commercial salt, allowing an average energy penetration of 62 W/m^2 to the storage layer.

The design goals selected by Edesess et al. (1979) for their hypothetical pond consisted of maintaining a temperature difference (storage versus ambient), ΔT , of 60°C , while meeting an average thermal demand, L , of $2.8 \times 10^5 \text{ W}$. These constraints were substituted into Eq. 4-13, allowing the required pond radius r to be obtained as a function of the average energy penetration to the storage layer, \bar{E}_p . A plot of this relationship appears as Fig. 5-2. Note that at a certain energy penetration rate, 30 W/m^2 in this case, the required pond radius approaches infinity. Below this minimum rate, the pond is unable to maintain the required average difference between storage layer and ambient temperatures. The transmittance of the EPS solution (as tested) is low enough that a gradient pond constructed of such material to meet the given design constraints would of necessity be impractically large. However, modifications to the sample testing protocol, as well as modifications to the solutions to be used to construct the ponds, may result in more optimistic predictions of the utility of alternate salts (see Error Analysis, Sec. 6.0).

This discussion demonstrates that optical transmittance of the upper layers of a gradient pond has a very significant effect upon the thermal performance of the pond, limiting both the available thermal output and the storage layer temperature. Even given an initially clean salt, upper-layer transparency can decrease during pond operation for numerous reasons. Further study of these phenomena is clearly warranted to hasten the commercialization of salt gradient solar ponds.

5.6 SPECTRAL TRANSMITTANCE OF MIAMISBURG POND SOLUTION SAMPLES

Attempts to make similar predictions of energy penetration for the Miamisburg, Ohio, pond based on absorbance spectra from samples of the pond solution have failed to date because the absorbances measured for samples having different concentrations do not conform to Beer's law in the visible region. Measurement errors are believed to be responsible for the discrepancies (see Error

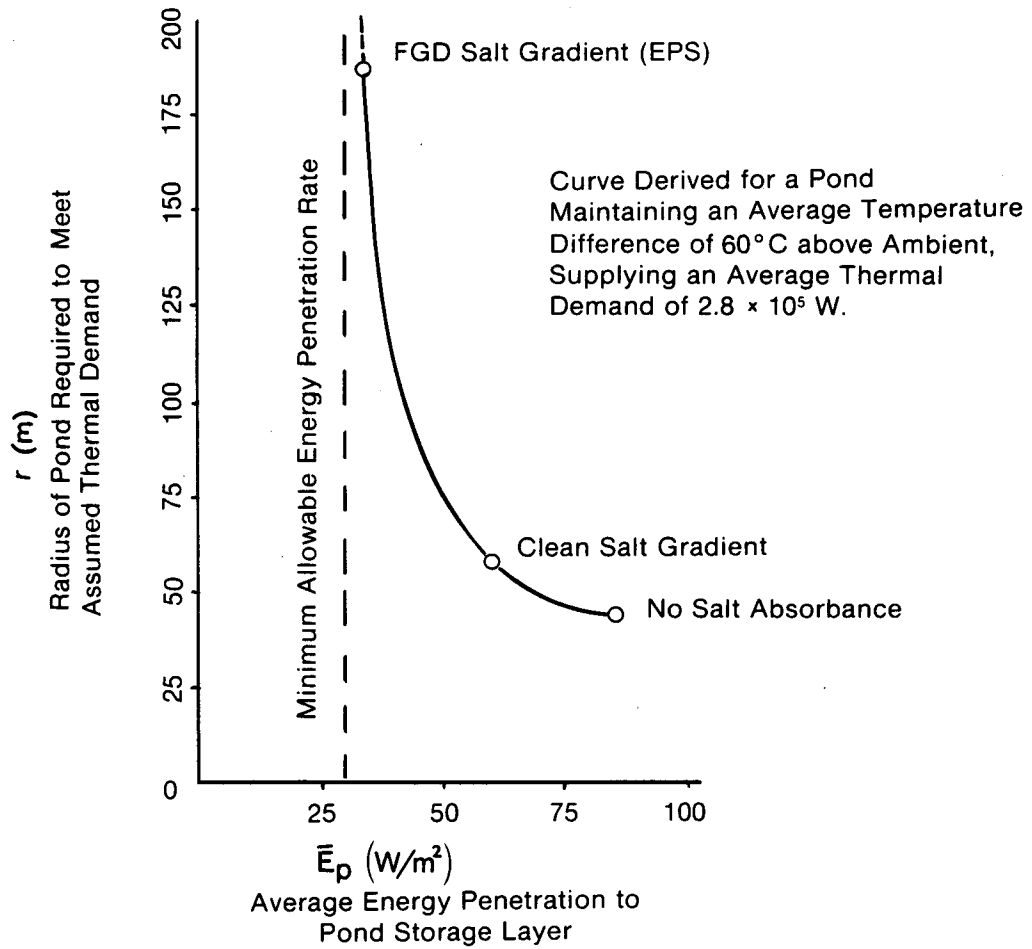


Figure 5-2. Dependence of Design Radius of a Typical Solar Pond On Average Energy Penetration

Analysis, Sec. 6.0). Refinement of the measurement technique should make possible an interesting comparison between program PON predictions and energy penetration measurements currently being made at Miamisburg by Monsanto, Inc., using a submersible radiometer. However, a general statement that the solutions are quite transparent relative to the FGD solutions can be made based on the obtained spectra. The samples, taken at various depths in the pond, all showed transmissions of 95%-99% from 400-800 nm in the 10-cm cells. The spectra recorded for these samples (unboiled and unfiltered) are reproduced as Figs. 5-3, 5-4, and 5-5.

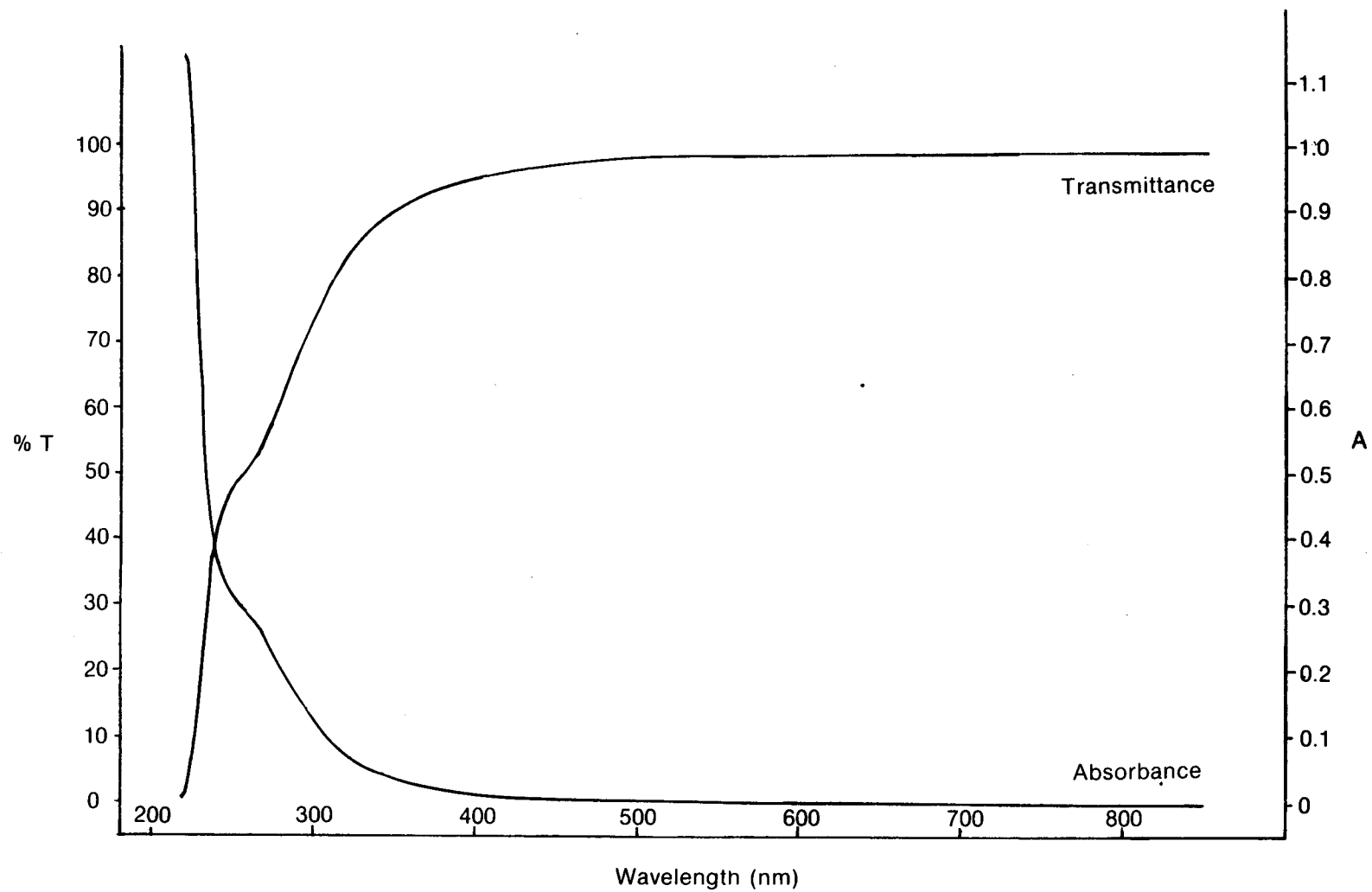


Figure 5-3. Transmittance and Absorbance Spectra of Miamisburg Pond Solution Sampled at 0.3-M Depth (NaCl Concentration + 1.40% (wt.), Optical Path Length = 10.0 cm (Sampled 5/79))

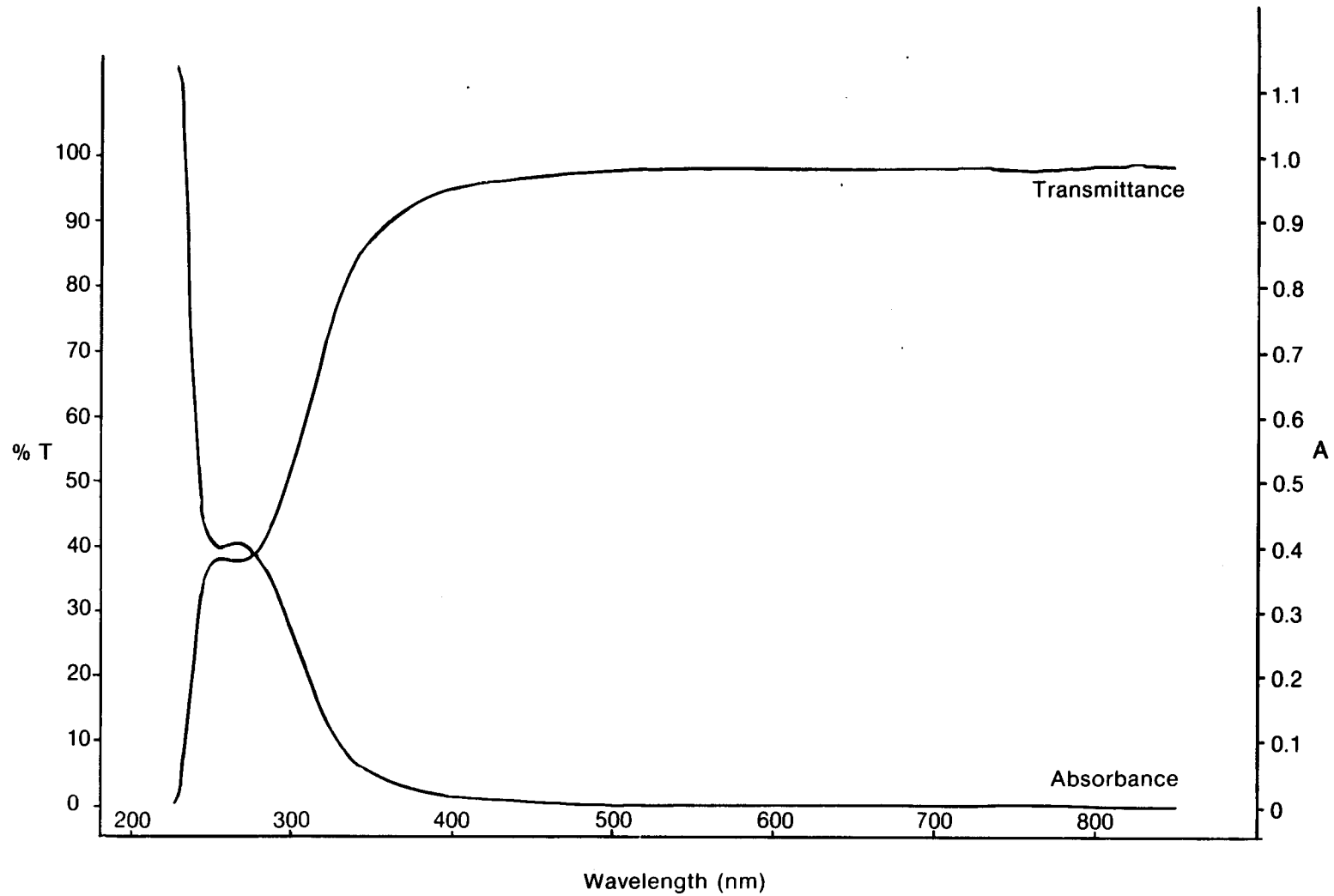


Figure 5-4. Transmittance and Absorbance Spectra of Miamisburg Pond Solution Sampled at 1.2-M Depth (NaCl Concentration = 4.50% (wt.), Optical Path Length = 10.0 cm (Sampled 5/79))

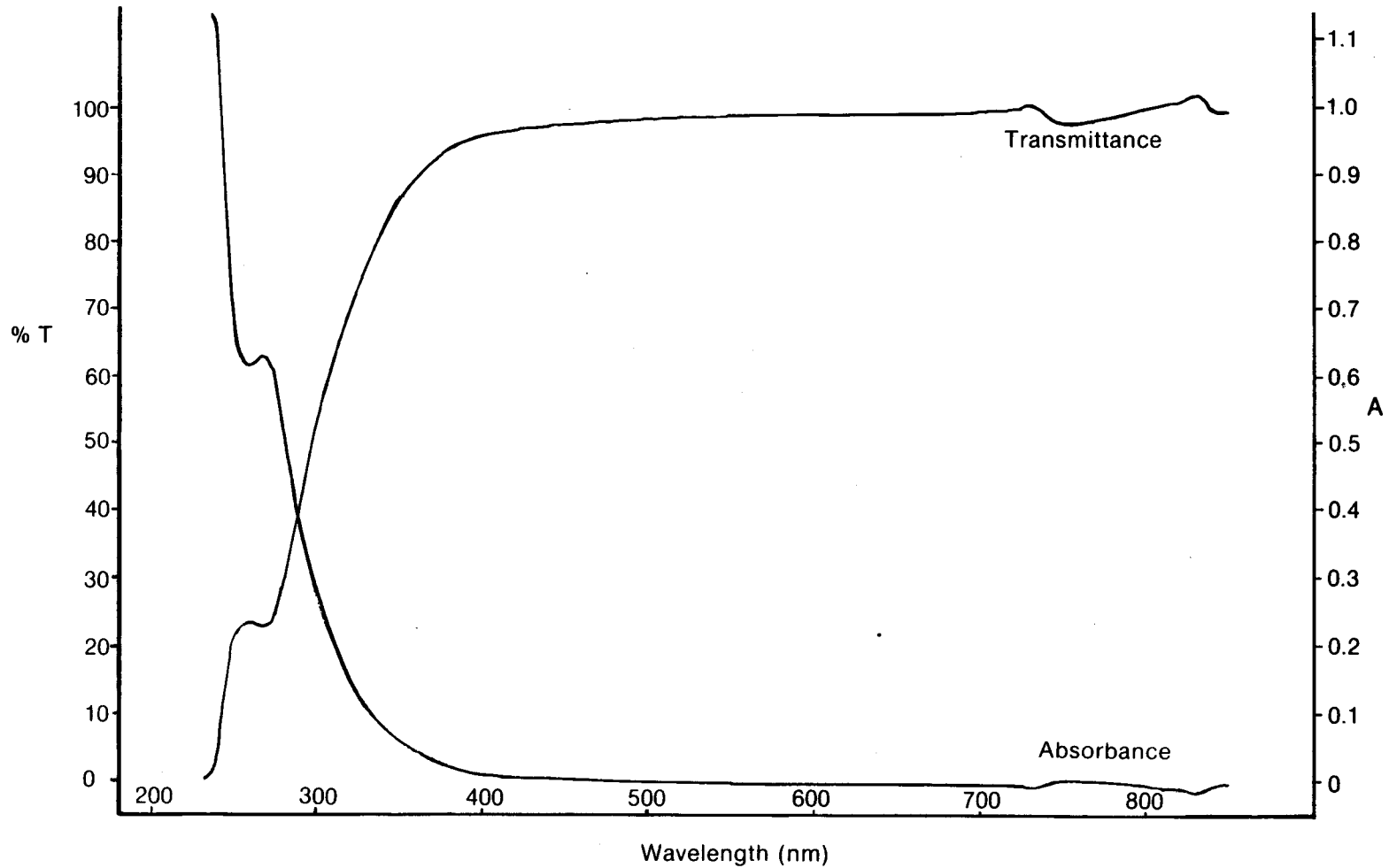


Figure 5-5. Transmittance and Absorbance Spectra of Miamisburg Pond Solution Sampled at 3.0-M Depth (NaCl Concentration = 18.9% (wt.), Optical Path Length = 10.0 cm (Sampled 5/79))

SERIO 

SECTION 6.0

ERROR ANALYSIS

Three major sources of error in the spectral transmittance measurements taken to date have been identified. These are: the presence of dissolved air in the samples (molecular scattering), the presence of particulate matter in the samples (bulk scattering), and nonreproducible sample cell alignment. Estimates for the quantitative effect of molecular scattering and of cell alignment on the transmittance measurements have been made.

The effect of dissolved air will be considered first. In Fig. 6-1, dual-beam transmittance spectra taken on 10-cm cells containing deionized water are reproduced. The upper plot appearing in this figure represents the transmittance ratio of two cells containing boiled water. The lower plot resulted from substitution of air-saturated water for the boiled water in the sample cell. For the air-saturated sample, an increase of 0.02-0.05 transmittance units, relative to the boiled water sample, is observable between 850 and 340 nm. The gradual increase in the apparent absorption of the air-saturated water (from which bubbles had been removed ultrasonically) towards the blue end of the spectrum indicates that the absorbance measured for this sample is probably a spurious effect related to scattering of the sampling beam by dissolved air molecules. Any light scattered from the samples at an angle greater than the acceptance angle of the spectrophotometer detector optics will appear as absorbance on the instrument readout. Predictions of energy penetration based on such measurements will generally be low, since light scattered in a forward direction can still penetrate to the storage layer of a pond.

The FGD and Miamisburg solute samples were probably not saturated with air. However, an increase in transmittance of up to 0.005 units in the visible region was observed. A Miamisburg sample (0.3-m depth) was boiled and remeasured, indicating the presence of sufficient dissolved air in the original sample to affect the measurement. The FGD salt solutions were not boiled before the transmission measurements were made. Therefore, the extinction coefficients reported for these salts in Table 5-5 may be spuriously high. The extinction coefficients measured for water will not include this error since the water was boiled before measurement. In summary, the effect of dissolved air in the samples will be to reduce the measured transmittance by as much as 0.05 units, although for the FGD salts, a reduction of 0.005 units is more likely.

A similar effect could have been caused by the presence of particulate matter in the samples tested. The only precaution taken to remove particulate matter from the samples was to let them stand for several days before withdrawing aliquots from the upper portion of the samples for measurement of transmittance. This procedure was probably inadequate to remove finely divided ferric hydroxide. No attempt to estimate the effect of particulate scattering on the FGD salt measurements was made.

In addition to the errors in transmittance caused by air particulates, random errors in the measurements are thought to have been introduced by

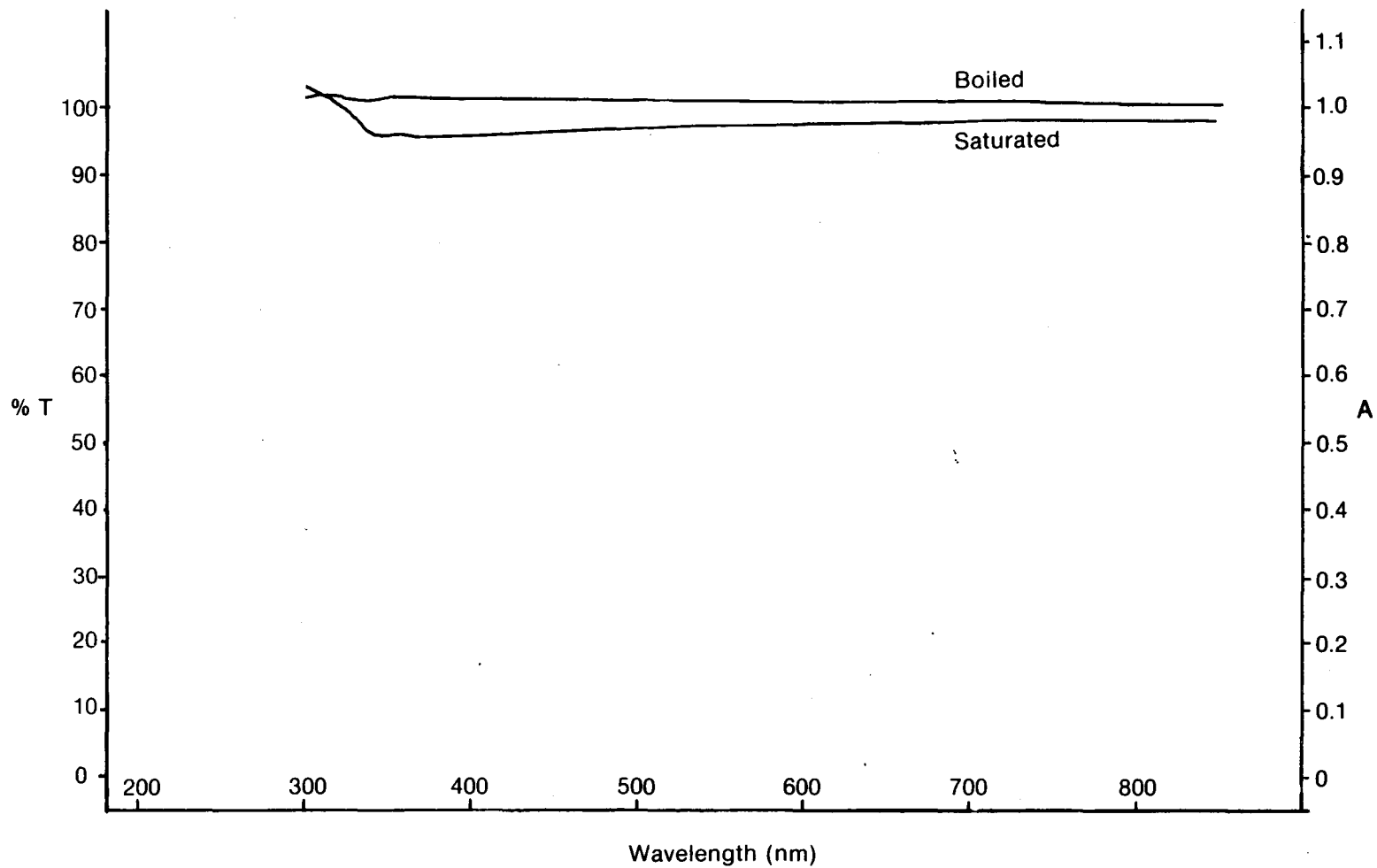


Figure 6-1. Spectra of Boiled, Deionized Water and Air-Saturated, Deionized Water vs. Boiled, Deionized Water as a Reference (Spectra Taken Using 10-cm Quartz Cells)

nonreproducible positioning of the sample and reference cells in their holders. This type of error is a possible explanation for the zero and negative absorbance values recorded for the FGD and Miamisburg salt solutions (see Table 5-5).

The cell holders used could be positioned reproducibly along the lateral and longitudinal axis, but rotation about the longitudinal axis of the cells can occur. Rotation of the sample cell by 45° produced variations in the percentage of light transmitted of ±0.01 transmittance units at 550 nm.

Examination of the cells in a darkened room using a helium-neon laser revealed several low-angle (<2°) scattering centers on the faces of the cells. Rotation of the cells while in the sample compartment of the spectrophotometer evidently caused variations in the amount of light scattered away from the detector, resulting in fluctuations in apparent cell transmittance. Prior to sample measurements, the cells were routinely filled with deionized water and a baseline spectrum taken. The cell in the sample beam path was then removed, filled with the sample under study, and replaced. Any variation in cell position introduced at this time could result in a random error in the recorded sample absorbance.

These investigations indicate that the error in the measured salt and water transmittances is on the order of ±0.01 transmittance units, a quantity which is greater than the instrumental reproducibility by a factor of ten. The effect of such errors on the energy penetration predictions may be estimated by expressing the predicted pond light transmission in terms of the measured sample transmittances, taking the partial derivative with respect to each measured transmittance, forming the total derivative, and integrating over the solar spectrum to obtain the perturbation in transmitted energy. Insufficient data are available to allow statistical analyses of variance. Equation 4-8 may be written:

$$I_1 = I_0 \exp [-\Delta d_1(\epsilon_1 c_1 + \epsilon_2 c_2)] \quad (6-1)$$

for two light-absorbing species at concentrations c_1 and c_2 that are constant over a depth Δd_1 in the pond. To obtain this equation in terms of the transmittance actually observed in the spectrophotometer, the substitution

$$\epsilon_n = -\ln (T_n/c_{sn}l_{sn}) \quad (6-2)$$

may be made, where T_n is the transmittance fraction obtained for species n at a given wavelength, c_{sn} is the concentration of species n in the sample, and l_{sn} is the effective path length of the sample. Equation 6-1 then becomes:

$$I_1 = I_0 \exp \Delta d \left(\frac{\ln T_1 c_1}{c_{s1} l_{s1}} + \frac{\ln T_2 c_2}{c_{s2} l_{s2}} \right) \quad (6-3)$$

The partial derivatives of 6-3 with respect to T_1 and T_2 are:

$$\left(\frac{\partial I_1}{\partial T_1} \right)_{T_2} = \frac{I_0 \Delta d c_1}{c_{s1} l_{s1} T_1} \exp \Delta d \left(\frac{\ln T_1 c_1}{c_{s1} l_{s1}} + \frac{\ln T_2 c_2}{c_{s2} l_{s2}} \right), \quad (6-4)$$

$$\left(\frac{\partial I_1}{\partial T_2}\right)_{T_1} = \frac{I_0 \Delta d c_2}{c_{s2} \lambda_{s2} T_2} \exp \Delta d \left(\frac{\ln T_1 c_1}{c_{s1} \lambda_{s1}} + \frac{\ln T_2 c_2}{c_{s2} \lambda_{s2}} \right) \quad (6-5)$$

For simplicity, Eqs. 6-4 and 6-5 may be written in terms of the extinction coefficients, again making use of Eq. 6-2:

$$\left(\frac{\partial I_1}{\partial T_1}\right)_{T_1} = \frac{-I_0 \Delta d c_1}{c_{s1} \lambda_{s1}} \exp -(\Delta d \epsilon_1 c_1 + \Delta d \epsilon_2 c_2 + \lambda_{s1} \epsilon_1 c_{s1}) \quad (6-6)$$

$$\left(\frac{\partial I_1}{\partial T_2}\right)_{T_2} = \frac{-I_0 \Delta d c_2}{c_{s2} \lambda_{s2}} \exp -(\Delta d \epsilon_1 c_1 + \Delta d \epsilon_2 c_2 + \lambda_{s2} \epsilon_2 c_{s2}) \quad (6-7)$$

The total differential dI_1 may be approximated, making use of Eq. 6-6 and 6-7, as follows:

$$\Delta I_1 \approx \left(\frac{\partial I_1}{\partial T_1}\right)_{T_2} \Delta T_1 + \left(\frac{\partial I_1}{\partial T_2}\right)_{T_1} \Delta T_2 \quad (6-8)$$

This equation can be solved at discrete wavelengths for a given set of pond and sample parameters to yield an estimate for the error ΔI_1 incurred in predicting light transmitted to pond depth Δd , resulting from sample transmittance measurement errors of ΔT_1 or ΔT_2 . However, some qualitative interpretations of Eqs. 6-6 and 6-7 will be made first. Holding other variables constant, the error of the predicted light penetration into the pond increases with solar spectral intensity, pond depth, and species concentration in the pond. Predictive errors will be reduced by increasing the sample species concentration and sample optical path length. The exponential portions of Eqs. 6-6 and 6-7 predict that error will be greatest at wavelengths where the species extinction coefficients are smallest, i.e., where the samples are most transparent.

To estimate the magnitude of the error in energy penetration predicted by program PON by thorough use of Eq. 6-8, representative parameters of the experimental conditions were chosen. Evaluation of the error at $\Delta d = 100$ cm will permit determination of the error in predicted energy input to the storage layer of the hypothetical pond having the profile measured at OSU. Depth-weighted average values for the concentration of salt and water in the pond (c_1 and c_2) were used to approximate the salinity gradient over the 100-cm interval. Values for λ_{s1} and λ_{s2} representing the longest sample cell paths were chosen, although the extinction coefficients presented for the FGD salts represent averages taken over several cell path lengths. The values for ΔT_1 and ΔT_2 were taken as ± 0.01 transmittance units.

These parameters, in addition to others, used in evaluating Eq. 6-8, are presented in Table 6-1.

Table 6-1. SELECTED CONSTANTS FOR ERROR ANALYSIS UTILIZING EQ. 6-8

$c_1 = 989.7$ g/L	$c_2 = 67.0$
$c_{s1} = 997.0$ g/L	$c_{s2} = 100.0$ g/L
$\lambda_{s1} = 9.00$ cm	$\lambda_{s2} = 10.00$ cm
$\Delta d = 100.0$ cm	$\Delta T_1 = \Delta T_2 = 0.01$

Equation 6-8 was evaluated at 0.100-micron intervals between 0.300 and 1.000 micron. At wavelengths longer than 1.000 micron, the intensity of light transmitted through one meter of solution becomes negligibly small. The results are summarized in Table 6-2.

To determine the error in the total energy transmitted to depth $\Delta d = 100$ cm resulting from errors in measured transmittance (ΔT_1 and ΔT_2) of ± 0.01 , the following integrals must be evaluated:

$$\Delta E_{T_1}(1) = \int_{\lambda_1}^{\lambda_2} \left(\frac{\partial I_1}{\partial T_1} \right)_{T_2} \Delta T_1 d\lambda \quad , \quad (6-9)$$

$$\Delta E_{T_2}(1) = \int_{\lambda_1}^{\lambda_2} \left(\frac{\partial I}{\partial T_2} \right)_{T_1} \Delta T_2 d\lambda \quad . \quad (6-10)$$

The maximum predicted error in the transmitted energy can be determined by summing the individual errors:

$$\Delta E_{\max}(1) = \Delta E_{T_1}(1) + \Delta E_{T_2}(1) \quad . \quad (6-11)$$

However, if the transmittance errors are truly random (i.e., sample cell alignment errors predominate over scattering errors), the most probable predicted error is the rms error:

$$\Delta E_{\text{prob}}(1) = \pm [(\Delta E_{T_1}(1))^2 + (\Delta E_{T_2}(1))^2]^{1/2} \quad . \quad (6-12)$$

These error boundaries may be expressed as percentages of either the transmitted or the incident energy. The latter approach is consistent with the mode of presentation of program PON results in Fig. 5-1. Approximate solutions to Eqs. 6-9 and 6-10 may be obtained by numerical integration using the trapezoidal method. If $\Delta\lambda$ is set equal to 100 nm, data from Table 6-2 may be used to evaluate the integrals. Virtually all of the energy transmitted is encompassed by the wavelength interval 300-1000 nm, making analysis over any broader limits unnecessary.

Table 6-3 is a summary of the results of error function integration over each 100-nm wavelength interval between 300 and 1000 nm. The incident and transmitted energies calculated from Table 9 data, and the transmitted energy and

Table 6-2. ERROR IN SPECTRAL INTENSITY, I_1 , PREDICTED AT A DEPTH OF ONE METER FOR A POND HAVING THE EPS CONCENTRATION GRADIENT GIVEN IN TABLE 5-6

λ (μm)	ϵ_1 (L/g-cm)	ϵ_2 (L/g-cm)	I_0 (W/m ² - μm)	I_1 (W/m ² - μm)	$\left(\frac{\partial I_1}{\partial T_1}\right)_{T_2} \Delta T_1$ (W/m ² - μm)	$\left(\frac{\partial I_1}{\partial T_2}\right)_{T_1} \Delta T_2$ (W/m ² - μm)	ΔI_1 (W/m ² - μm)
0.300	1.90×10^{-6}	2.00×10^{-3}	0.660	8.2×10^{-7}	$\mp 1.3 \times 10^{-7}$	$\mp 9. \times 10^{-8}$	$\mp 2.2 \times 10^{-7}$
0.400	1.30×10^{-7}	3.00×10^{-4}	621.9	8.2×10^1	$\mp 1.3 \times 10^1$	$\mp 9. \times 10^0$	$\mp 2.2 \times 10^1$
0.500	1.70×10^{-7}	1.01×10^{-4}	1248.0	6.2×10^2	$\mp 9.6 \times 10^1$	$\mp 7. \times 10^1$	$\mp 1.7 \times 10^2$
0.600	1.50×10^{-6}	4.08×10^{-5}	1262.0	8.3×10^2	$\mp 1.3 \times 10^2$	$\mp 9. \times 10^1$	$\mp 2.2 \times 10^2$
0.700	3.75×10^{-6}	1.80×10^{-5}	1173.0	7.2×10^2	$\mp 1.1 \times 10^2$	$\mp 8. \times 10^1$	$\mp 1.9 \times 10^2$
0.800	2.00×10^{-5}	1.20×10^{-5}	988.1	1.3×10^2	$\mp 2. \times 10^1$	$\mp 1. \times 10^1$	$\mp 3. \times 10^1$
0.900	6.10×10^{-5}	0.00	807.8	1.9×10^0	$\mp 3. \times 10^{-1}$	$1. \times 10^{-1}$	$\mp 4. \times 10^{-1}$
1.000	4.76×10^{-4}	1.01×10^{-5}	536.8	1.7×10^{-18}	$\mp 3. \times 10^{-19}$	$3. \times 10^{-21}$	$\mp 3. \times 10^{-19}$

Table 6-3. SENSITIVITY OF PREDICTED SOLAR ENERGY TRANSMITTED TO THE STORAGE LAYER OF AN EPS SOLAR POND TO A 1% ERROR IN LABORATORY-MEASURED SOLUTION TRANSMITTANCE

Wavelength Interval		Incident Energy	Energy Transmitted to 100-cm Depth	Sensitivity to $\Delta T_1 = \pm 0.01$ (water)	Sensitivity to $\Delta T_2 = \pm 0.01$ (FGD Salt Solution)	Maximum Sensitivity	rms Sensitivity
$\lambda_1 \rightarrow \lambda_2$	E_o	$E_T(1)$	$\Delta E_{T_1}(1)$	$\Delta E_{T_2}(1)$	$\Delta E_{max}(1)$	$\Delta E_{prob}(1)$	
(μm)	(W/m^2)	(W/m^2)	(W/m^2)	(W/m^2)	(W/m^2)	(W/m^2)	(W/m^2)
0.300 0.400	31.0	4.1	± 0.5	± 0.2	± 0.7	± 0.5	
0.400 0.500	94.0	35.0	± 4.0	± 2.9	± 6.0	± 4.0	
0.500 0.600	130.0	73.0	± 8.0	± 5.0	± 13.0	± 9.0	
0.600 0.700	120.0	77.0	± 8.0	± 5.0	± 13.0	± 9.0	
0.700 0.800	110.0	42.0	± 4.0	± 3.0	± 13.0	± 5.0	
0.800 0.900	90.0	6.4	± 0.6	± 0.4	± 1.0	± 0.7	
0.900 1.000	67.0	0.10	± 0.01	± 0.01	± 0.02	± 0.1	
Total from 0.300-1.000 μm (Rounded)		640.0	240.0	± 25.0	± 16.0	± 41.0	± 28.0

33

error sums over the 300-1000 nm interval are also given. The result for total energy transmitted to 100 cm differs slightly from that shown in Fig. 5-1 for the EPS solution, since the depth-weighted concentration average used in evaluating Eq. 6-8 is not an accurate representation of the concentration gradient.

Some interesting conclusions may be drawn from the data presented in Table 6-3 (page 34). Over 95% of the energy transmitted to the storage layer of this hypothetical solar pond falls in the wavelength "window" between 0.4 and 0.8 microns. For this reason, the total energy penetration prediction is almost entirely insensitive to errors made outside the "window," and accurate measurement of sample transmittance within this range is of primary importance.

The error analysis also shows that when cell alignment is the major source of error in sample transmittance measurement, errors in measuring the transmittance of the pure water samples represent the controlling factor in the rms measurement error. However, if the salt solutions cause significant light scattering, the scattering error could easily dominate the analysis, and the maximum errors reported are likely to apply.

For the chosen conditions, the errors as percentages of incident and transmitted energy are reported in Table 6-4. The PON result for total incident energy from 0.300-2.500 μm , 819 W/m^2 , was used for E_0 .

Table 6-4. ERROR BOUNDARIES ON PROGRAM PON PREDICTIONS

(Incident Energy Available Calculated from the A.M.-1.5 Solar Spectrum was 819 W/m^2)

Program PON Prediction	Maximum Error	rms Error
Percentage of Incident Energy (E_0) Transmitted	29% \pm 5%	29% \pm 3%
Transmitted Energy	240 W/m^2 \pm 41 W/m^2	240 W/m^2 \pm 28 W/m^2

It is evident from an examination of Eqs. 6-6 and 6-7 that several other factors possibly contributing to error in this analysis were not considered. Differences in $I_0(\lambda)$, the tabulated solar spectral distribution, can cause significant shifts in the predicted energy penetration profile for a pond. Such differences occur as a result of daily and seasonal variations in sun angle and atmospheric conditions, or because of differences in measurement techniques. Errors in measured sample concentrations and optical path lengths were assumed to be insignificant. Finally, the estimates for ΔT_1 and ΔT_2 are open to some doubt. However, the primary purpose of this error analysis was to determine the feasibility of predicting the optical performance of a solar pond based on laboratory measurements of solution transmittance. Recommendations for improving the accuracy of such predictions, based on the results of this analysis, appear in the following two sections.

SECTION 7.0

CONCLUSIONS

- Visible light transmittance of the upper layers of a gradient pond is a key parameter controlling performance.
- Although preliminary results indicate that the FGD salts, as tested, would be inferior in optical performance to commercially available salt for pond gradient construction, these analyses suggest that the salts may be useable if some relatively simple precautions are taken. For example, a series of FGD salt processing ponds similar to the one at the Utah plant, with a high pH effluent-settling pond interconnected to an evaporating pond, should produce salt that is virtually iron-free. Additional measures such as heating or ultrasonic agitation could be taken to ensure complete flocculation of precipitates in the effluent pond. For dry FGD residues, which contain fly ash as well as soluble salt, such treatment could be undertaken in the solar pond itself, since a gradient-stabilized pond affords an excellent environment for settling of dense solids.
- In general, the pH of gradient-stabilized ponds should be kept high to allow transition metal ions to precipitate. Levels of only a few parts per million of iron or copper ion, dissolved in the upper layers of a pond, are sufficient to reduce significantly the energy transmitted to the storage layer of the pond.
- The Miamisburg pond samples were only slightly less transparent than pure water in the visible region of the solar spectrum.
- An error analysis indicates that the results predicted for energy penetration to a pond storage layer, using an FGD salt gradient, were accurate to about $\pm 12\%$ (rms, absolute), if no scattering occurred during the sample transmittance measurements. Several options exist for improving the accuracy of the analytical procedure used to determine the salt extinction coefficients. Salt solutions to be analyzed should be nearly saturated. Before spectral analysis, the salt solution should be boiled to drive off dissolved air and to flocculate any precipitates. The liquid samples should then be cooled to room temperature anaerobically and tested for pH. Any adjustments to the pH made at this point should duplicate those to be done in the actual pond. The sample then should be hydraulically pressure-filtered using a 0.25 micron (or smaller) micropore filter to simulate the eventual settling of precipitates in the pond. Sample cell holders permitting reproducible cell alignment must be used. The critical wavelength range for the measurement of salt extinction coefficients is 400-800 nm; the minimum usable optical pathlength for measurements in this range is 10 cm.

The procedure should be repeated several times for each sample, and the results should be analyzed for mean and variance.

SERIO 

SECTION 8.0

WORK IN PROGRESS

- To decrease the effect of cell alignment errors, a frosted quartz scatter plate has been placed in front of the photomultiplier detector in the Perkin-Elmer Model 340 spectrophotometer. If this approach proves ineffective, an integrating sphere (recently completed) may be used in conjunction with the cells.
- Dish pressure filters with syringe pumps for removing particles above 0.25 microns in diameter have been obtained. These will be used to prefilter samples for analysis.
- Fresh samples of FGD salts and salt solutions sampled from operating gradient ponds will be obtained and subjected to analysis with the proposed improvements. If variance of these results is unacceptably high, an attempt to design and build a 100-cm liquid cell will be made.
- After a number of salts have been screened in this manner, a promising candidate will be selected to establish a gradient in one of the 3-m outdoor testing tanks erected at the SERI Mangone Testing Facility. Measurements of incident energy and energy penetration profiles into the tank will be carried out using the Gamma Scientific Model DR-2 spectroradiometer recently purchased. An immersible fiber-optic probe three meters in length is now being constructed and calibrated for this purpose. The outdoor measurements will include the effects of surface reflectance, sun angle, and particulates, as well as those of soluble contaminants. These measurements will constitute final acceptance tests for salts to be used in constructing gradient ponds at the SERI permanent field testing site.

SERI 

SECTION 9.0

REFERENCES

- Brandhorst, Jr., H. W. et al. 1977. Terrestrial Photovoltaic Measurement Procedures. NASA TM 73702; ERDA/NASA/1022-77/16. Cleveland, OH: NASA-Lewis Research Center.
- Edesess, M.; Henderson, J.; Jayadev, T. S. 1979 (Dec.). A Simple Design Tool for Sizing Solar Ponds. SERI/RR-351-347. Golden, CO: Solar Energy Research Institute.
- Nielsen, C. 1976. "Experience with a Prototype Solar Pond for Space Heating." Winnipeg Conference Proceedings. Vol. 5: pp. 169-182.
- Querry, M. R. et al. 1977 (Mar. 20). "Relative Reflectance and Complex Refractive Index in the Infrared for Saline Environmental Waters." Journal of Geophysical Research. Vol. 3 (No. 9): pp. 1425-33.
- Washburn, E. W. (Ed.). 1929. International Critical Tables of Numerical Data, Physics, Chemistry, and Technology. Vol. 5. NY: McGraw-Hill; p. 269.
- Weast, Robert C. (Ed.). 1969. Handbook of Chemistry and Physics. 49th ed., p. D-177; Chemical Rubber Company.

SERIO 

APPENDIX A

PROGRAM PON OUTPUT LISTINGS

Reproduced here are outputs of the PON solar energy penetration analyses as performed on pure water, standard solutions containing Cu^{+2} and Fe^{+3} , and two EPS solutions having different concentration profiles.

CONTENTS:

<u>PON Analysis</u>	<u>Section</u>
Pure water, 1-m depth, $\Delta d = 1$ cm.	B-1
Cu^{+2} , 1-m depth, $\Delta d = 1$ cm.	B-2
Fe^{+3} , 1-m depth, $\Delta d = 1$ cm.	B-3
Pure water, 2.3-m depth, $\Delta d = 1$ cm, 5 cm.	B-4
EPS, OSU profile, 2.3-m depth, $\Delta d = 1$ cm, 5 cm.	B-5
EPS, Edesess' profile, 2.3-m depth, $\Delta d = 1$ cm, 5 cm.	B-6

1	2	3	4	5	6	7	1	2	3	4	5	6	7
1.000	0.000	997.000	160.517	19.507	160.517	19.507	1.000	5.000	997.000	161.115	19.581	161.115	19.581
2.000	0.000	997.000	36.389	4.445	196.965	24.052	2.000	5.000	997.000	36.329	4.499	197.464	24.179
3.000	0.000	997.000	21.737	2.655	218.543	26.708	3.000	5.000	997.000	22.117	2.702	200.050	25.391
4.000	0.000	997.000	15.553	1.600	234.196	28.608	4.000	5.000	997.000	15.896	1.942	235.956	28.323
5.000	0.000	997.000	12.292	1.002	246.488	30.109	5.000	5.000	997.000	12.600	1.540	248.561	30.362
6.000	0.000	997.000	10.265	1.254	256.754	31.363	6.000	5.000	997.000	10.555	1.289	259.117	31.452
7.000	0.000	997.000	8.866	1.083	265.620	32.444	7.000	5.000	997.000	9.136	1.116	268.253	32.768
8.000	0.000	997.000	7.835	.957	273.455	33.408	8.000	5.000	997.000	8.088	.988	276.341	33.756
9.000	0.000	997.000	7.042	.860	280.447	34.263	9.000	5.000	997.000	7.250	.889	282.621	34.445
10.000	0.000	997.000	6.413	.783	286.916	35.047	10.000	5.000	997.000	6.637	.811	290.258	35.456
11.000	0.000	997.000	5.900	.721	292.819	35.767	11.000	5.000	997.000	6.112	.747	295.370	36.202
12.000	0.000	997.000	5.474	.669	298.294	36.436	12.000	5.000	997.000	5.675	.693	302.045	36.995
13.000	0.000	997.000	5.114	.625	303.399	37.061	13.000	5.000	997.000	5.305	.648	307.350	37.544
14.000	0.000	997.000	4.805	.587	308.204	37.648	14.000	5.000	997.000	4.986	.609	312.336	38.153
15.000	0.000	997.000	4.536	.554	312.739	38.202	15.000	5.000	997.000	4.708	.575	317.044	38.728
16.000	0.000	997.000	4.299	.525	317.038	38.727	16.000	5.000	997.000	4.463	.545	321.507	39.270
17.000	0.000	997.000	4.088	.499	321.126	39.226	17.000	5.000	997.000	4.244	.518	325.751	39.791
18.000	0.000	997.000	3.899	.475	325.024	39.702	18.000	5.000	997.000	4.048	.494	329.799	40.286
19.000	0.000	997.000	3.728	.455	328.752	40.158	19.000	5.000	997.000	3.870	.472	333.654	40.759
20.000	0.000	997.000	3.572	.436	332.324	40.594	20.000	5.000	997.000	3.708	.452	337.377	41.211
21.000	0.000	997.000	3.430	.419	335.754	41.013	21.000	5.000	997.000	3.560	.435	340.937	41.646
22.000	0.000	997.000	3.299	.403	339.053	41.416	22.000	5.000	997.000	3.428	.421	344.359	42.064
23.000	0.000	997.000	3.178	.388	342.239	41.804	23.000	5.000	997.000	3.299	.408	347.656	42.467
24.000	0.000	997.000	3.065	.374	345.295	42.179	24.000	5.000	997.000	3.179	.395	350.835	42.855
25.000	0.000	997.000	2.960	.362	348.225	42.540	25.000	5.000	997.000	3.066	.382	353.904	43.230
26.000	0.000	997.000	2.862	.350	351.112	42.880	26.000	5.000	997.000	2.960	.369	356.870	43.592
27.000	0.000	997.000	2.770	.339	353.938	43.228	27.000	5.000	997.000	2.870	.357	359.740	43.943
28.000	0.000	997.000	2.684	.329	356.702	43.556	28.000	5.000	997.000	2.790	.340	362.520	44.283
29.000	0.000	997.000	2.602	.318	359.414	43.874	29.000	5.000	997.000	2.720	.329	365.214	44.612
30.000	0.000	997.000	2.525	.308	362.099	44.182	30.000	5.000	997.000	2.613	.319	367.827	44.931
31.000	0.000	997.000	2.452	.300	364.751	44.482	31.000	5.000	997.000	2.537	.310	370.364	45.241
32.000	0.000	997.000	2.383	.291	367.334	44.773	32.000	5.000	997.000	2.464	.301	372.828	45.542
33.000	0.000	997.000	2.317	.283	369.850	45.056	33.000	5.000	997.000	2.394	.293	375.223	45.834
34.000	0.000	997.000	2.254	.275	372.310	45.331	34.000	5.000	997.000	2.329	.285	377.553	46.119
35.000	0.000	997.000	2.194	.268	374.729	45.599	35.000	5.000	997.000	2.267	.277	379.819	46.396
36.000	0.000	997.000	2.137	.261	377.109	45.860	36.000	5.000	997.000	2.207	.270	382.026	46.665
37.000	0.000	997.000	2.083	.254	379.459	46.115	37.000	5.000	997.000	2.150	.263	384.176	46.928
38.000	0.000	997.000	2.031	.248	381.780	46.365	38.000	5.000	997.000	2.095	.256	386.271	47.184
39.000	0.000	997.000	1.980	.242	384.081	46.609	39.000	5.000	997.000	2.043	.250	388.314	47.433
40.000	0.000	997.000	1.932	.236	386.363	46.841	40.000	5.000	997.000	1.992	.243	390.306	47.677
41.000	0.000	997.000	1.885	.230	388.627	47.071	41.000	5.000	997.000	1.944	.237	392.250	47.914
42.000	0.000	997.000	1.842	.225	390.871	47.296	42.000	5.000	997.000	1.899	.232	394.148	48.146
43.000	0.000	997.000	1.800	.220	393.091	47.516	43.000	5.000	997.000	1.853	.226	396.002	48.372
44.000	0.000	997.000	1.759	.215	395.294	47.731	44.000	5.000	997.000	1.811	.221	397.812	48.594
45.000	0.000	997.000	1.719	.210	397.468	47.941	45.000	5.000	997.000	1.769	.215	399.582	48.810
46.000	0.000	997.000	1.681	.205	399.614	48.146	46.000	5.000	997.000	1.730	.211	401.311	49.021
47.000	0.000	997.000	1.644	.201	401.734	48.347	47.000	5.000	997.000	1.692	.207	403.003	49.228
48.000	0.000	997.000	1.609	.197	403.829	48.544	48.000	5.000	997.000	1.655	.202	404.658	49.430
49.000	0.000	997.000	1.575	.192	405.900	48.736	49.000	5.000	997.000	1.619	.198	406.277	49.628
50.000	0.000	997.000	1.542	.188	407.950	48.924	50.000	5.000	997.000	1.585	.194	407.862	49.821
51.000	0.000	997.000	1.510	.184	409.980	49.109	51.000	5.000	997.000	1.552	.190	409.413	50.011
52.000	0.000	997.000	1.479	.181	409.950	49.290	52.000	5.000	997.000	1.520	.186	410.933	50.196
53.000	0.000	997.000	1.450	.177	409.959	49.467	53.000	5.000	997.000	1.489	.182	412.422	50.379
54.000	0.000	997.000	1.421	.174	409.950	49.640	54.000	5.000	997.000	1.459	.178	413.880	50.556
55.000	0.000	997.000	1.393	.170	409.923	49.810	55.000	5.000	997.000	1.430	.175	415.310	50.730
56.000	0.000	997.000	1.365	.167	409.874	49.977	56.000	5.000	997.000	1.402	.171	416.712	50.902
57.000	0.000	997.000	1.340	.164	410.809	50.141	57.000	5.000	997.000	1.375	.168	418.087	51.070
58.000	0.000	997.000	1.315	.161	411.733	50.301	58.000	5.000	997.000	1.348	.165	419.435	51.235
59.000	0.000	997.000	1.290	.158	412.633	50.454	59.000	5.000	997.000	1.323	.162	420.758	51.397
60.000	0.000	997.000	1.266	.155	413.509	50.614	60.000	5.000	997.000	1.298	.159	422.057	51.555
61.000	0.000	997.000	1.243	.152	415.353	50.765	61.000	5.000	997.000	1.274	.156	423.331	51.711
62.000	0.000	997.000	1.221	.149	416.314	50.915	62.000	5.000	997.000	1.251	.153	424.582	51.864
63.000	0.000	997.000	1.199	.146	418.013	51.061	63.000	5.000	997.000	1.229	.150	425.811	52.014
64.000	0.000	997.000	1.178	.144	419.190	51.205	64.000	5.000	997.000	1.207	.147	427.018	52.161
65.000	0.000	997.000	1.157	.141	420.348	51.346	65.000	5.000	997.000	1.186	.145	428.204	52.306
66.000	0.000	997.000	1.138	.139	421.485	51.485	66.000	5.000	997.000	1.165	.142	429.369	52.448
67.000	0.000	997.000	1.118	.137	422.604	51.622	67.000	5.000	997.000	1.145	.140	430.515	52.588
68.000	0.000	997.000	1.099	.134	423.703	51.755	68.000	5.000	997.000	1.125	.138	431.641	52.726
69.000	0.000	997.000	1.081	.132	424.784	51.885	69.000	5.000	997.000	1.107	.135	432.748	52.861
70.000	0.000	997.000	1.063	.130	425.847	52.013	70.000	5.000	997.000	1.089	.133	433.838	52.994
71.000	0.000	997.000	1.044	.128	426.894	52.146	71.000	5.000	997.000	1.071	.131	434.909	53.125
72.000	0.000	997.000	1.024	.126	427.923	52.272	72.000	5.000	997.000	1.054	.129	435.962	53.254
73.000	0.000	997.000	1.013	.124	428.936	52.395	73.000	5.000	997.000	1.037	.127	436.999	53.380
74.000	0.000	997.000	.997	.122	429.933	52.517	74.000	5.000	997.000	1.021	.125	438.019	53.505
75.000	0.000	997.000	.982	.120	430.914	52.637	75.000	5.000	997.000	1.005	.123	439.024	53.628
76.000	0.000	997.000	.966	.118	431.881	52.755	76.000	5.000	997.000	.989	.121	440.013	53.749
77.000	0.000	997.000	.952	.116	432.833	52.871	77.000	5.000	997.000	.974	.119	440.987	53.868
78.000	0.000	997.000	.938	.115	433.770	52.984	78.000	5.000	997.000	.959	.117	441.947	53.985
79.000	0.000	997.000	.924	.113	434.694	53.099	79.000	5.000	997.000	.945	.115	442.892	54.100
80.000	0.000	997.000	.910	.111	435.604	53.210							

1	2	3	4	5	6	7
1.000	.100	997.000	150.525	19.421	150.525	19.621
2.000	.100	997.000	39.439	4.453	197.124	34.079
3.000	.100	997.000	21.945	2.565	215.963	26.747
4.000	.100	997.000	15.650	1.713	234.629	28.650
5.000	.100	997.000	12.396	1.214	247.027	30.175
6.000	.100	997.000	10.371	1.027	257.399	31.442
7.000	.100	997.000	8.971	1.096	266.369	32.533
8.000	.100	997.000	7.939	.970	274.308	33.507
9.000	.100	997.000	7.145	.873	281.453	34.380
10.000	.100	997.000	6.515	.796	287.963	35.176
11.000	.100	997.000	6.002	.733	293.969	35.909
12.000	.100	997.000	5.575	.681	299.545	36.590
13.000	.100	997.000	5.214	.637	304.759	37.227
14.000	.100	997.000	4.904	.599	309.663	37.826
15.000	.100	997.000	4.634	.566	314.297	38.392
16.000	.100	997.000	4.396	.537	318.694	38.929
17.000	.100	997.000	4.185	.511	322.879	39.446
18.000	.100	997.000	3.995	.488	326.874	39.933
19.000	.100	997.000	3.823	.467	330.699	40.395
20.000	.100	997.000	3.667	.448	334.365	40.843
21.000	.100	997.000	3.524	.430	337.889	41.274
22.000	.100	997.000	3.392	.414	341.281	41.688
23.000	.100	997.000	3.271	.400	344.552	42.088
24.000	.100	997.000	3.157	.386	347.709	42.473
25.000	.100	997.000	3.052	.373	350.761	42.846
26.000	.100	997.000	2.953	.361	353.714	43.207
27.000	.100	997.000	2.861	.349	356.575	43.556
28.000	.100	997.000	2.773	.339	359.348	43.895
29.000	.100	997.000	2.691	.329	362.039	44.224
30.000	.100	997.000	2.613	.319	364.653	44.543
31.000	.100	997.000	2.540	.310	367.193	44.853
32.000	.100	997.000	2.470	.302	369.663	45.155
33.000	.100	997.000	2.403	.294	372.066	45.449
34.000	.100	997.000	2.340	.286	374.406	45.735
35.000	.100	997.000	2.280	.278	376.686	46.013
36.000	.100	997.000	2.222	.271	378.908	46.284
37.000	.100	997.000	2.167	.265	381.075	46.549
38.000	.100	997.000	2.114	.258	383.189	46.807
39.000	.100	997.000	2.063	.253	385.252	47.059
40.000	.100	997.000	2.015	.246	387.267	47.305
41.000	.100	997.000	1.968	.240	389.235	47.546
42.000	.100	997.000	1.923	.235	391.159	47.781
43.000	.100	997.000	1.880	.230	393.033	48.010
44.000	.100	997.000	1.838	.225	394.876	48.235
45.000	.100	997.000	1.798	.220	396.675	48.455
46.000	.100	997.000	1.760	.215	398.435	48.670
47.000	.100	997.000	1.723	.210	400.157	48.880
48.000	.100	997.000	1.687	.206	401.844	49.086
49.000	.100	997.000	1.652	.202	403.496	49.288
50.000	.100	997.000	1.619	.198	405.115	49.486
51.000	.100	997.000	1.586	.194	406.701	49.679
52.000	.100	997.000	1.555	.190	408.255	49.869
53.000	.100	997.000	1.525	.186	409.781	50.056
54.000	.100	997.000	1.495	.183	411.276	50.233
55.000	.100	997.000	1.467	.179	412.743	50.417
56.000	.100	997.000	1.439	.176	414.182	50.593
57.000	.100	997.000	1.413	.173	415.595	50.766
58.000	.100	997.000	1.387	.169	416.982	50.935
59.000	.100	997.000	1.362	.166	418.344	51.102
60.000	.100	997.000	1.338	.163	419.681	51.265
61.000	.100	997.000	1.314	.161	420.995	51.425
62.000	.100	997.000	1.291	.158	422.286	51.583
63.000	.100	997.000	1.269	.155	423.555	51.738
64.000	.100	997.000	1.247	.152	424.802	51.891
65.000	.100	997.000	1.226	.150	426.028	52.040
66.000	.100	997.000	1.206	.147	427.234	52.189
67.000	.100	997.000	1.186	.145	428.420	52.333
68.000	.100	997.000	1.167	.143	429.587	52.475
69.000	.100	997.000	1.148	.140	430.735	52.615
70.000	.100	997.000	1.130	.138	431.865	52.753
71.000	.100	997.000	1.112	.136	432.977	52.889
72.000	.100	997.000	1.095	.134	434.072	53.023
73.000	.100	997.000	1.078	.132	435.150	53.155
74.000	.100	997.000	1.062	.130	436.212	53.284
75.000	.100	997.000	1.046	.128	437.259	53.412
76.000	.100	997.000	1.030	.126	438.293	53.539
77.000	.100	997.000	1.015	.124	439.303	53.662
78.000	.100	997.000	1.000	.122	440.303	53.784
79.000	.100	997.000	.986	.120	441.289	53.904
80.000	.100	997.000	.972	.119	442.261	54.023
81.000	.100	997.000	.958	.117	443.220	54.140
82.000	.100	997.000	.945	.115	444.165	54.256
83.000	.100	997.000	.932	.114	445.097	54.370
84.000	.100	997.000	.919	.112	446.016	54.482
85.000	.100	997.000	.907	.111	446.923	54.593
86.000	.100	997.000	.895	.109	447.818	54.702
87.000	.100	997.000	.883	.108	448.701	54.810
88.000	.100	997.000	.872	.106	449.573	54.916
89.000	.100	997.000	.860	.105	450.433	55.021
90.000	.100	997.000	.849	.104	451.289	55.125
91.000	.100	997.000	.839	.102	452.131	55.228
92.000	.100	997.000	.828	.101	452.950	55.329
93.000	.100	997.000	.818	.100	453.768	55.429
94.000	.100	997.000	.808	.099	454.576	55.527
95.000	.100	997.000	.798	.098	455.374	55.625
96.000	.100	997.000	.789	.096	456.163	55.721
97.000	.100	997.000	.779	.095	456.942	55.816
98.000	.100	997.000	.770	.094	457.712	55.911
99.000	.100	997.000	.761	.093	458.473	56.004
100.000	.100	997.000	.752	.092	459.226	56.095

COLUMN 1 = SOIL DEPTH (CM)
 COLUMN 2 = SALT CONCENTRATION (G/L) AT MIDPOINT OF PRECEDING DEPTH INTERVAL
 COLUMN 3 = WATER CONCENTRATION (G/L) AT MIDPOINT OF PRECEDING DEPTH INTERVAL
 COLUMN 4 = ENERGY (G-CM) ABSORBED IN PRECEDING DEPTH INTERVAL
 COLUMN 5 = PER CENT OF AVAIL. ENERGY ABSORBED IN PRECEDING DEPTH INTERVAL
 COLUMN 6 = CUMULATIVE ENERGY (G-CM) ABSORBED AT DEPTH 1
 COLUMN 7 = CUMULATIVE PER CENT OF AVAIL. ENERGY ABSORBED

B-3. Fe^{+3} , 1-m depth, $\Delta d = 1$ cm

1	2	3	4	5	6	7
1.000	0.000	997.000	160.517	19.607	160.517	19.607
2.000	0.000	997.000	36.389	4.445	196.906	24.052
3.000	0.000	997.000	21.737	2.655	218.643	26.708
4.000	0.000	997.000	15.553	1.900	234.196	28.608
5.000	0.000	997.000	12.292	1.502	246.488	30.109
6.000	0.000	997.000	10.265	1.254	256.754	31.363
7.000	0.000	997.000	8.866	1.083	265.620	32.446
8.000	0.000	997.000	7.835	.957	273.455	33.403
9.000	0.000	997.000	7.042	.860	280.497	34.263
10.000	0.000	997.000	6.413	.783	286.910	35.047
15.000	0.000	997.000	25.829	3.155	312.739	38.202
20.000	0.000	997.000	19.585	2.392	332.324	40.594
25.000	0.000	997.000	15.931	1.946	348.255	42.540
30.000	0.000	997.000	13.443	1.642	361.699	44.182
35.000	0.000	997.000	11.600	1.417	373.299	45.599
40.000	0.000	997.000	10.163	1.241	383.463	46.841
45.000	0.000	997.000	9.006	1.100	392.468	47.941
50.000	0.000	997.000	8.052	.984	400.520	48.924
55.000	0.000	997.000	7.253	.886	407.773	49.810
60.000	0.000	997.000	6.577	.803	414.350	50.614
65.000	0.000	997.000	5.998	.733	420.348	51.346
70.000	0.000	997.000	5.500	.672	425.847	52.018
75.000	0.000	997.000	5.067	.619	430.914	52.637
80.000	0.000	997.000	4.689	.573	435.604	53.210
85.000	0.000	997.000	4.358	.532	439.962	53.742
90.000	0.000	997.000	4.066	.497	444.029	54.239
95.000	0.000	997.000	3.808	.465	447.836	54.704
100.000	0.000	997.000	3.578	.437	451.414	55.141
105.000	0.000	997.000	3.373	.412	454.788	55.553
110.000	0.000	997.000	3.189	.390	457.977	55.943
115.000	0.000	997.000	3.024	.369	461.001	56.312
120.000	0.000	997.000	2.876	.351	463.877	56.664
125.000	0.000	997.000	2.741	.335	466.619	56.999
130.000	0.000	997.000	2.619	.320	469.238	57.318
135.000	0.000	997.000	2.508	.306	471.746	57.625
140.000	0.000	997.000	2.407	.294	474.154	57.919
145.000	0.000	997.000	2.315	.283	476.469	58.202
150.000	0.000	997.000	2.230	.272	478.699	58.474
155.000	0.000	997.000	2.152	.263	480.851	58.737
160.000	0.000	997.000	2.081	.254	482.932	58.991
165.000	0.000	997.000	2.014	.246	484.946	59.237
170.000	0.000	997.000	1.953	.239	486.899	59.476
175.000	0.000	997.000	1.896	.232	488.795	59.707
180.000	0.000	997.000	1.843	.225	490.638	59.933
185.000	0.000	997.000	1.794	.219	492.432	60.152
190.000	0.000	997.000	1.748	.214	494.180	60.365
195.000	0.000	997.000	1.705	.208	495.885	60.573
200.000	0.000	997.000	1.664	.203	497.549	60.777
205.000	0.000	997.000	1.626	.199	499.175	60.975
210.000	0.000	997.000	1.590	.194	500.766	61.170
215.000	0.000	997.000	1.557	.190	502.323	61.360
220.000	0.000	997.000	1.525	.186	503.847	61.546
225.000	0.000	997.000	1.494	.183	505.342	61.729
230.000	0.000	997.000	1.466	.179	506.807	61.908

COLUMN 1 = POND DEPTH (CM)
 COLUMN 2 = SALT CONCENTRATION (G/L) AT MIDPOINT OF PRECEDING DEPTH INTERVAL
 COLUMN 3 = WATER CONCENTRATION (G/L) AT MIDPOINT OF PRECEDING DEPTH INTERVAL
 COLUMN 4 = ENERGY (W/M2) ABSORBED IN PRECEDING DEPTH INTERVAL
 COLUMN 5 = PER CENT OF AVAIL. ENERGY ABSORBED IN PRECEDING DEPTH INTERVAL
 COLUMN 6 = CUMULATIVE ENERGY (W/M2) ABSORBED AT DEPTH 1
 COLUMN 7 = CUMULATIVE PER CENT OF AVAIL. ENERGY ABSORBED

B-4. Pure water, 2.3-m depth, $A_d = 1$ cm, 5 cm

1	2	3	4	5	6	7
1.000	25.500	995.500	161.620	19.742	161.620	19.742
2.000	25.500	995.500	37.542	4.586	199.161	24.328
3.000	25.500	995.500	22.877	2.794	222.038	27.122
4.000	25.500	995.500	16.677	2.037	238.715	29.160
5.000	25.500	995.500	13.401	1.637	252.116	30.797
6.000	25.500	995.500	11.362	1.388	263.478	32.184
7.000	25.500	995.500	9.950	1.215	273.428	33.400
8.000	25.500	995.500	8.908	1.088	282.336	34.488
9.000	25.500	995.500	8.103	.990	290.439	35.478
10.000	25.500	995.500	7.463	.912	297.901	36.389
15.000	25.500	995.500	30.923	3.777	328.824	40.167
20.000	25.500	995.500	24.436	2.985	353.260	43.152
25.000	25.500	995.500	20.562	2.512	373.822	45.663
30.000	25.500	995.500	17.871	2.183	391.693	47.846
35.000	25.500	995.500	15.841	1.935	407.534	49.781
40.000	25.500	995.500	14.231	1.738	421.765	51.520
45.000	25.500	995.500	12.913	1.577	434.678	53.097
50.000	36.995	993.447	13.536	1.653	448.214	54.750
55.000	49.767	991.167	14.277	1.744	462.491	56.494
60.000	62.539	988.886	14.872	1.817	477.363	58.311
65.000	75.311	986.605	15.297	1.869	492.660	60.179
70.000	88.082	984.325	15.549	1.899	508.209	62.079
75.000	100.854	982.044	15.642	1.911	523.851	63.990
80.000	113.626	979.763	15.594	1.905	539.444	65.894
85.000	126.398	977.482	15.424	1.884	554.868	67.778
90.000	139.170	975.202	15.151	1.851	570.019	69.629
95.000	151.942	972.921	14.792	1.807	584.811	71.436
100.000	164.714	970.640	14.363	1.755	599.175	73.191
105.000	171.604	969.383	13.530	1.653	612.704	74.843
110.000	172.612	969.148	12.429	1.518	625.134	76.361
115.000	173.619	968.913	11.457	1.400	636.591	77.761
120.000	174.627	968.679	10.592	1.294	647.183	79.055
125.000	175.635	968.444	9.817	1.199	657.001	80.254
130.000	176.642	968.210	9.120	1.114	666.121	81.368
135.000	177.650	967.975	8.490	1.037	674.611	82.405
140.000	178.658	967.740	7.917	.967	682.528	83.372
145.000	179.665	967.506	7.396	.903	689.924	84.276
150.000	180.673	967.271	6.920	.845	696.844	85.121
155.000	181.681	967.037	6.483	.792	703.327	85.913
160.000	182.688	966.802	6.082	.743	709.409	86.656
165.000	183.696	966.567	5.712	.698	715.121	87.354
170.000	184.704	966.333	5.371	.656	720.492	88.010
175.000	185.712	966.098	5.056	.618	725.548	88.627
180.000	186.719	965.863	4.763	.582	730.311	89.209
185.000	187.727	965.629	4.491	.549	734.803	89.758
190.000	188.735	965.394	4.239	.518	739.041	90.276
195.000	189.742	965.160	4.003	.489	743.045	90.765
200.000	190.750	964.925	3.783	.462	746.828	91.227
205.000	191.758	964.690	3.578	.437	750.406	91.664
210.000	192.765	964.456	3.386	.414	753.792	92.077
215.000	193.773	964.221	3.206	.392	756.998	92.469
220.000	194.781	963.987	3.037	.371	760.035	92.840
225.000	195.788	963.752	2.878	.352	762.913	93.192
230.000	196.796	963.517	2.729	.333	765.642	93.525

COLUMN 1 = POND DEPTH (CM)
 COLUMN 2 = SALT CONCENTRATION (G/L) AT MIDPOINT OF PRECEDING DEPTH INTERVAL
 COLUMN 3 = WATER CONCENTRATION (G/L) AT MIDPOINT OF PRECEDING DEPTH INTERVAL
 COLUMN 4 = ENERGY (W/M²) ABSORBED IN PRECEDING DEPTH INTERVAL
 COLUMN 5 = PER CENT OF AVAIL. ENERGY ABSORBED IN PRECEDING DEPTH INTERVAL
 COLUMN 6 = CUMULATIVE ENERGY (W/M²) ABSORBED AT DEPTH 1
 COLUMN 7 = CUMULATIVE PER CENT OF AVAIL. ENERGY ABSORBED

B-5. EPS, OSU profile, 2.3-m depth, $\Delta d = 1$ cm, 5 cm

1	2	3	4	5	6	7
1.000	25.500	995.500	161.620	19.742	161.620	19.742
2.000	25.500	995.500	37.542	4.586	199.161	24.328
3.000	25.500	995.500	32.377	2.794	222.039	27.122
4.000	25.500	995.500	16.677	2.037	233.715	29.160
5.000	25.500	995.500	13.401	1.637	252.116	30.797
6.000	25.500	995.500	11.362	1.388	263.478	32.184
7.000	25.500	995.500	9.950	1.215	273.428	33.400
8.000	25.500	995.500	9.303	1.089	282.336	34.483
9.000	25.500	995.500	8.103	.990	290.434	35.478
10.000	25.500	995.500	7.463	.912	297.901	36.399
15.000	25.500	995.500	30.423	3.777	328.824	40.167
20.000	25.500	995.500	24.435	2.965	353.260	43.152
25.000	25.500	995.500	20.562	2.512	373.822	45.663
30.000	25.500	995.500	17.871	2.183	391.693	47.846
35.000	29.533	994.953	16.349	1.997	408.041	49.843
40.000	34.600	993.275	15.671	1.914	423.713	51.757
45.000	40.667	992.792	15.163	1.852	438.875	53.610
50.000	46.733	991.709	14.749	1.802	453.624	55.411
55.000	52.800	990.625	14.389	1.757	468.012	57.169
60.000	58.867	989.542	14.053	1.717	482.055	58.885
65.000	64.933	988.457	13.739	1.677	495.797	60.563
70.000	71.000	987.375	13.414	1.639	509.211	62.201
75.000	77.067	986.292	13.095	1.600	522.307	63.801
80.000	83.133	985.208	12.774	1.560	535.090	65.361
85.000	89.200	984.125	12.447	1.520	547.528	66.882
90.000	95.267	983.042	12.115	1.480	559.643	68.362
95.000	101.333	981.958	11.777	1.439	571.420	69.800
100.000	107.400	980.875	11.434	1.397	582.854	71.197
105.000	113.467	979.792	11.086	1.354	593.940	72.551
110.000	119.533	978.708	10.735	1.311	604.675	73.862
115.000	125.600	977.625	10.380	1.268	615.055	75.130
120.000	131.667	976.542	10.024	1.224	625.078	76.355
125.000	137.733	975.458	9.667	1.181	634.745	77.536
130.000	143.800	974.375	9.311	1.137	644.055	78.673
135.000	149.867	973.292	8.955	1.094	653.012	79.767
140.000	155.933	972.208	8.600	1.051	661.617	80.819
145.000	162.000	971.125	8.259	1.009	669.876	81.827
150.000	168.067	970.042	7.917	.967	677.793	82.794
155.000	174.133	968.958	7.567	.917	685.300	83.711
160.000	179.200	967.875	7.205	.861	692.350	84.572
165.000	185.267	966.792	6.830	.810	699.050	85.382
170.000	191.333	965.708	6.440	.762	705.290	86.144
175.000	197.400	964.625	6.030	.718	711.100	86.862
180.000	203.467	963.542	5.600	.677	716.645	87.540
185.000	209.533	962.458	5.154	.639	721.879	88.179
190.000	215.600	961.375	4.694	.604	726.823	88.783
195.000	221.667	960.292	4.223	.571	731.494	89.354
200.000	227.733	959.208	3.743	.540	735.916	89.894
205.000	233.800	958.125	3.253	.511	740.099	90.405
210.000	239.867	957.042	2.753	.484	744.050	90.889
215.000	245.933	955.958	2.243	.458	747.812	91.347
220.000	252.000	954.875	1.723	.434	751.369	91.781
225.000	258.067	953.792	1.193	.412	754.742	92.193
230.000	264.133	952.708	0.653	.391	757.941	92.584

COLUMN 1 = BOND DEPTH (CM).
 COLUMN 2 = SALT CONCENTRATION (G/KG) AT MIDPOINT OF PRECEDING DEPTH INTERVAL.
 COLUMN 3 = WATER CONCENTRATION (G/KG) AT MIDPOINT OF PRECEDING DEPTH INTERVAL.
 COLUMN 4 = ENERGY (CM²) ABSORBED IN PRECEDING DEPTH INTERVAL.
 COLUMN 5 = PER CENT OF AVAIL. ENERGY ABSORBED IN PRECEDING DEPTH INTERVAL.
 COLUMN 6 = CUMULATIVE ENERGY (CM²) ABSORBED AT DEPTH 1.
 COLUMN 7 = CUMULATIVE PER CENT OF AVAIL. ENERGY ABSORBED.

B-6. EPS, Edesess' profile, 2.3-m depth, $\Delta d = 1$ cm, 5 cm

Document Control Page	1. SERI Report No. RR-641-615	2. NTIS Accession No.	3. Recipient's Accession No.
4. Title and Subtitle Optical Transparency of Inexpensive Salt Solutions for Construction of Density-Gradient Solar Ponds		5. Publication Date July 1981	
7. Author(s) John D. Webb		6.	
9. Performing Organization Name and Address Solar Energy Research Institute 1617 Cole Blvd Golden, Colorado 80401		8. Performing Organization Rept. No.	
		10. Project/Task/Work Unit No. 1089.00	
		11. Contract (C) or Grant (G) No. (C) (G)	
12. Sponsoring Organization Name and Address		13. Type of Report & Period Covered Research Report	
		14.	
15. Supplementary Notes			
16. Abstract (Limit: 200 words) A laboratory testing protocol has been developed that will permit a comparative evaluation of the optical performance of candidate salts for use in stabilizing solar ponds. Extinction coefficients measured for the salts and for water in dual-beam spectrophotometer fitted with 10-cm quartz sample cells were input to a digital model that convolutes a solar spectrum with an assumed salt/water concentration gradient similar to that to be established in the solar pond. The model determined the fraction of available solar energy transmitted to the pond storage layer. This information was used to estimate the size of the pond needed to meet a given set of thermal demands if the candidate salt were to be used. One candidate salt, a by-product from a flue-gas desulfurization process, was tested according to this protocol. Results indicated that this salt would perform poorly in comparison to commercially available sodium chloride; however, a sensitivity analysis revealed sources of error in the spectrophotometric measurement procedure, which may have led to an unduly pessimistic prediction of performance. These errors are being corrected, and this and other candidate salts will be subject to further evaluation for use in ponds to be constructed on-site.			
17. Document Analysis			
a. Descriptors absorption ; copper ; iron ; magnesium ; salts ; sodium chloride ; solar ponds			
b. Identifiers/Open-Ended Terms flue-gas desulfurization salts ; light transmittance			
c. UC Categories 62a, b, e			
18. Availability Statement National Technical Information Service U.S. Department of Commerce 5285 Port Royal Road Springfield, Virginia 22161		19. No. of Pages 50	
		20. Price \$4.50	



National Renewable
Energy Laboratory



02LIB094350

